Modelling and Performance Investigation of Anode-off Gas Combustion in an IC Engine for Power Generation

By

S.M. Krol

in partial fulfilment of the requirements for the degree of

Master of Science
in Marine Technology

at the Delft University of Technology,
to be defended publicly on 27-08, 2018 at Delft

Supervisor:	Ir. H. Sapra
Thesis committee:	Ir. K. Visser
	Dr. Ir. M. Godjevac
	Prof. Dr. D.J.E.M. Roekaerts

TU Delft

Abstract

In the GasDrive project, a solid oxide fuel cell and a reciprocating gas engine are used to provide electrical and mechanical power for a ship. One of the goals of the GasDrive project is to broaden the limits between knock and misfire for the gas engine. Extending the operating limit could be achieved by addition of anode-off gas. Before anode-off gas can be used in combustion together with natural gas in the GasDrive project, the combustion characteristics of anode-off gas must be known. In this thesis, a literature review is conducted in order to explore similar gasses. One such gas is producer gas, on which both experimental and numerical studies have been conducted by other researchers. To investigate the performance of anode-off gas, an altered in-cylinder model was used. The model is verified using producer gas as a fuel, with the experimental data from producer gas combustion in an IC engine. The model functions properly and is used to investigate anode-off gas combustion.

In modelling the combustion of anode-off gas, multiple parameters are kept constant and similar to that of producer gas. These parameters include the Vibe parameters, engine geometry, air excess ratio, T_1, p_1, and stoichiometric gas mass fraction from the previous cycle. The combustion duration relative to producer gas is modelled based on the ratio of turbulent flame speeds. This turbulent flame speed is a combination of laminar flame speed and turbulence intensity. At first the SOC is kept constant as well, only altering the EOC for different combustion durations. The maximum power output is 79 kWe for anode-off gas with a 50% fuel utilization rate. The maximum efficiency is 20%. The peak pressure is 104 bar, which is higher than for producer gas, but falls within the limits of what the engine can handle. The peak temperature is 2847 K, which is more than 700 K higher than producer gas. The engine, it is believed, can not handle this temperature. The lowest peak temperature is reached for anode-off gas with a 85% fuel utilization rate and is 2652 K. This is still outside normal engine operating temperatures. Combustion of anode-off gas under stoichiometric conditions in an IC engine is therefore not feasible. Increasing the air excess ratio could resolve this issue, but can not be done in the current model without having experimental data on anode-off gas. The fuel consumption is 6-18 times higher than conventional fuels, also showing that anode-off gas combustion would not be an advantage over conventional fuels. More power at lower temperatures can be reached when retarding start of combustion, achieving MBT timing. Peak power is achieved using anode-off gas with a 50% fuel utilization rate and is 82 kWe. The corresponding peak temperature is 2822 K, which is also outside normal operating conditions of IC engines. Based on the modelling results, it can be said that combustion of anode-off gas is possible in a IC engine, but power outputs will be lower than conventional fuels and fuel consumption will be higher.

Acknowledgements

I would first like to extend my sincere thanks to Ir. Harsh Sapra, my supervisor. The long discussions and meetings contributed very much to how the final work has shaped up. His eye for detail has made sure that I would always check and recheck results.

I would like to extend special thanks to Dr. Annand Shivapuji, who was willing to share his experimental data with me and answer any questions I had on his research.

Special thanks and love go to Emily Henry, who has supported me and kept me going for the last nine months, always patient and understanding, and putting up with my long nights working on this thesis. Her support has been indispensable.

Thanks are due to all others who have supported in a variety of ways.

Table of Contents

List of figures

List of tables

Nomenclature

Symbol	Name	Unit
a	Constant in Vibe function	-
afr	Air/fuel ratio	-
AOG	Anode-off gas	-
ATDC	After top dead center	-
bsfc	Brake specific fuel consumption	-
BTDC	Before top dead center	-
CI	Compression ignition	-
c_m	Piston velocity	m/s
CR	Compression ratio	-
D_b	Bore diameter	m
E	Energy	kJ
IC	Internal Combustion	-
k	Conductive heat transfer coefficient	J/m^2K
LCV	Lower calorific value	kJ/kg
LHV	Lower heating value	kj/kg
L_s	Stroke length	m
m	mass	kg
$\dot{m}$	Mass flow	kg/s
M	Molecular weight	Kg/kmol
MBT	Maximum brake torque	-
NG	Natural gas	-
p	pressure	kPa or bar
PG	Producer gas	-
$\dot{q}$	Heat flow per unit of mass	kW/kg
Q	Heat	kJ
$\dot{Q}$	Heat flow	kW
sfc	Specific fuel consumption	g/kWh
SI	Spark Ignition	-
T	Absolute temperature	K

Symbol	Name	Unit
α	Heat transfer coefficient	J/m^2K
δ	Flame thickness	M
Z	Non dimensional rate of combustion	-
η	efficiency	-

λ	Air excess ratio	-
λ	Heat conduction coefficient	J/m^2K
ν	Kinematic viscosity	cSt
ζ	Reaction rate	Kg/s
ρ	density	Kg/m^3
σ	Stoichiometric air/fuel ratio	-
χ	Non-dimensional combustion progress	-

1 Introduction

1.1 Motivation

Most seagoing ships are still powered by diesel engines. But the growing concerns about environmental pollution, combined with stricter regulations on emissions for ships, have intensified the research into alternative fuels for internal combustion engines. One very effective way of reducing the diesel engine emissions is using gaseous fuels instead of diesel. The combustion of gaseous fuels results in almost no sulphur oxides (SO_x), relatively small amounts of nitrogen oxides (NO_x) and a substantial reduction in carbon dioxide (CO_2) compared to diesel engines. One of the studies into using gaseous fuels instead of conventional fossil diesel is the GasDrive project.

In the GasDrive project, a solid oxide fuel cell and a reciprocating gas engine are used to provide electrical and mechanical power for a ship. Usually gas engines are only used for generator applications due to their narrow window between knock and misfire. This narrow window restricts these types of engines from being used for direct propulsion of a ship, since they will not be able to cope with the transient loads. One way to broaden the limits between knock and misfire for the gas engine is adding hydrogen to the natural gas, which is currently being researched at the Delft University. Another way is to add anode-off gas. Even the use of anode-off gas as a sole fuel for power generation is a possibility.

Before adding anode-off gas to the gas engine, it is important to know what exactly the effect would be of adding anode-off gas. One of the ways to gain more knowledge about combusting anode-off gas is studying the combustion of anode-off gas by itself. A previous study determined that combusting the anode-off gas in an internal combustion engine is the most efficient use of the anode-off gas. The combustion of anode-off gas in an IC engine is, in broad terms, what will be researched in this thesis.

1.2 Problem statement

Anode-off gas combustion has not been studied before. There is no experimental data available, nor an engine model has been researched to predict powers, temperatures, pressures and more, for combustion of anode-off gas. The behaviour of anode-off gas combustion is therefore unknown. There are engine models available, and even one at the disposal of the author. However, this is a Diesel engine model, which is a compression ignition engine rather than a spark ignition engine. The latter is needed for combustion of anode-off gas. Also the addition of anode-off gas to natural gas in a regular gas engine model would not be feasible, because of the very different thermophysical properties of the two gasses.

The combustion characteristics of anode-off gas must be known before it can be used in combustion with natural gas. Therefore, this thesis aims to research the performance of an IC engine on different compositions of anode-off gas.

1.3 Goal and objectives

The goal of this Thesis can be stated as follows:

> *The goal of this Thesis is to research the performance of an IC engine on different compositions of anode-off gas, and if it can be used for power generation onboard of ships.*

Given the nature of this research, the goal is divided into two more specific objectives:

1. *Adjust an engine model which can be used for combustion of anode-off gas.*
2. *Investigate the performance of anode-off gas combustion.*

Several sub questions follow from the goal and objectives and will be answered throughout this thesis:

- *What is the composition of anode-off gas in comparison to similar gases?*
- *What do current studies say about gases with similar compositions in terms of efficiencies, flow rates, power derating, temperatures and emissions?*
- *What is the state-of-the-art for engines working with such gases?*
- *Which type of engine (SI or CI (Dual-fuel)) is the best choice?*
- *Which engine adjustments are needed to combust anode-off gas?*
- *Which input parameters are needed for the engine model?*
- *What type of engine modelling method would be suitable for this research?*
- *What are the in-cylinder pressures, temperatures, heat release rates, engine power, efficiency and specific fuel consumption for an engine on anode-off gas?*

1.4 Methodology

The methodology used in this thesis will now shortly be described. First of all, before adjusting an engine model and investigating the performance of an engine running on anode-off gas, more needs to be known about the gas. The specific properties of anode-off gas will be analysed in more detail

to get a better understanding of what might be needed. This includes the different constituents and their volume percentages, lower heating values and more.

The gas will then be compared to other gasses with similar properties, to develop an even better understanding of what could occur when combusting anode-off gas. This will be done through a literature study of several papers, books and other literature. Both experimental and numerical studies of similar gases to anode-off gas will be used to better understand the combustion of such a gas.

After more research into anode-off gas and similar gases, an existing engine model will be adjusted. The development of an engine model is a tedious task that takes a significant amount of time. Instead of building a completely new engine model, the Diesel-C model from Delft University of Technology will be used as a base model. This model will be converted to a gas engine by changing several parts of the model. Once this model is build, the model will be tested with available experimental data from other literature, using similar gases, to verify if the new model works correctly.

After the model has been verified, it will be used to investigate the performance of an engine running on anode-off gas. An engine from the literature study will be chosen as a base engine. From this engine, all data will be available, both on the engine as well as the gas used and the needed input parameters for the model. This will for example include the specific inlet conditions at the moment the inlet valve closes. The same engine will then be run in the model with anode-off gas. However, one important input parameter for the engine model is the combustion duration. Before anything valuable can be said about the combustion of anode-off gas, the combustion duration will have to be known. Since there is no straight forward way of determining this combustion duration, the combustion duration will be related to the flame speed of the gas. Both the flame speed and combustion durations of similar gases are known. The flame speed of anode-off gas can be calculated. Thus a link can be sought between the flame speed and combustion duration, with which the combustion duration for anode-off gas can be calculated.

The final step will be to run simulations of the model using anode-off gas. The in-cylinder pressures, temperatures, heat release rates, engine power, efficiency and specific fuel consumption will be compared to the same engine using another gas. With these results, the main question can be answered.

1.5 Thesis outline

The complete research is divided into seven different chapters. The first chapter introduces the motivation for this research, the problem statement and the goals which the author is trying to achieve. The second chapter looks more into anode-off gas, as well as comparable gasses and their properties, to get a better understanding of the behaviour of the gas as well as what has been done already in this field. Also, the engine type that is modelled, and the method to model this engine is chosen. The third chapter discusses the modifications needed to the Diesel-C model, before it can be used for anode-off gas combustion. In the fourth chapter the modified Diesel C model is matched with different experimental results from different studies. These studies use producer gas as fuel,

which is similar to anode-off gas. Matching of these experimental results would prove the model to work correctly. After verifying the model chapter five gives a more detailed picture of the behaviour of anode-off gas. The main difference between anode-off gas and producer gas is the H_2 content, which will have implications for the flame speed and combustion duration. Therefore, a way to predict the flame speed and combustion duration is investigated. Chapter six presents detailed results from the modelling of anode-off gas combustion. The conclusions and recommendations from this work can be found in chapter seven.

2 Literature Review

In the present study, the combustion of anode-off gas in an internal combustion engine will be simulated. The main components of anode-off gas are H_2, CO, CO_2 and H_2O. First more information on this gas will be given in this chapter. However, no study has been found where anode-off gas has been used in an IC engine. Therefore this literature review will further look into the combustion of synthesis gasses, also known as syngas or producer gas. This type of gas is an end product of gasification and consists mostly of the same components as anode-off gas. The properties of this gas will be researched and the studies and experiments done with this gas will be analysed. A comparison between anode-off gas and a similar gas will be made. In addition to analysing the combustion of synthesis gas and its challenges, this chapter will also investigate different modelling techniques to model the combustion of such a gas in order to predict the performance of an engine running on synthesis gas. A modelling technique as well as engine type to model will be chosen for the remaining part of this thesis. Emissions are not a main point of interest for this thesis, but will shortly be discussed in the light of the more strict regulations nowadays.

2-1 Properties of anode-off gas

The composition of anode-off gas is given in Table 1 for different fuel utilization rates. This anode-off gas comes from a solid oxide fuel cell as used in the GasDrive project.

Table 1: Composition of anode-off gas at different fuel utilization rates (volume percentages)

	85% fuel util.	**75% fuel util.**	**60% fuel util.**	**50% fuel util.**
H_2	14.8	24.3	37.95	46.63
CO	5.2	9.03	15.38	20.04
CO_2	28.13	24.3	17.95	13.29
H_2O	51.8	42.37	28.71	20.04

Before anode-off gas will go into an IC engine, the water will be taken out of the composition. This will change the volume percentages of the different constituents. This has been done, and also the lower calorific value of the different compositions has been calculated using the values from Table 1. An overview of this is given in **Fout! Verwijzingsbron niet gevonden.**

Table 2: Anode-off gas composition without H2O

		85% fuel util.	75% fuel util.	60% fuel util.	50% fuel util.
	H_2	30.75	42.17	53.24	58.32
	CO	10.80	15.67	21.58	25.06
	CO_2	58.45	42.17	25.18	16.62
LCV MJ/kg		38.31	52.62	66.62	73.12
LCV MJ/Nm^3		4.69	6.54	8.49	9.48

In most of the compositions of anode-off gas a relatively large amount of CO_2 is present. This inert gas brings the calorific value down. When looking at the LCV given in MJ/Nm^3, we see it is roughly between 4-9 MJ/Nm^3. This is the range of the lower calorific synthesis gas called producer gas. Also the volume percentages of combustible constituents is similar to producer gas (around 40-55 percent). However, the H_2 volume percentage is high compared to other experiments which will be discussed later on. This could change combustion properties and result in higher flame speeds and higher in-cylinder temperatures.

2-2 Properties of synthesis gas

Synthesis gas is an end product of gasification, a process in which carbonaceous materials are converted into H_2, CO and CO_2. It can be produced from different feedstock like coal, liquid hydrocarbons, biomass, and other waste products. The main gasifying agents used in the process are air, steam and oxygen. When the synthesis gas is produced using steam or oxygen, it is called medium calorific syngas, or simply syngas. When air is used, it is called lower calorific value gas, also known as producer gas (PG) [1]. The main constituents of synthesis gas are CO and H_2, with lesser amounts of CO_2 and CH_4. When air is the gasifying agent, around 50% of the composition is N_2. The combustible gasses are CO, H_2 and CH_4 and the non-combustible gasses are N_2 and CO_2. Varying proportions of these gasses can be present. The presence of nitrogen results in a lower calorific value, around 4-7 MJ/Nm^3, in which case the gas is called producer gas. When oxygen or steam is used in the process, the concentration of combustible components is significantly increased with lower calorific values up to 28 MJ/Nm^3, in which case it is called syngas [1]. The calorific value can be defined as the amount of heat that is released during combustion of one kg of fuel. However, the calorific value, or lower heating value, does not say it all as will be explained by the data from Table 3.

Table 3: Comparison of fuel properties, after [2], [3] and [4]

Fuel	LCV, MJ/kg (MJ/Nm^3)	Air/Fuel at φ=1, mass (mole)	Mixture, MJ/kg (MJ/Nm^3)	Flame speed S_L at φ=1, cm/s	Peak flame temperature, K	Product/reactant mole ratio
H_2	121 (10.8)	34.4 (3.2)	3.41 (3.2)	270	2400	0.67
CO	10.2 (12.7)	2.46 (2.38)	2.92 (3.8)	45	2400	0.67
CH_4	50.2 (35.8)	17.2 (9.52)	2.76 (3.4)	35	2210	1
Diesel ($C_{12}H_{26}$)	42	14.92	(2.82)	30	2290	
NG	45	18	(3)	35	2210	1
PG	5 (5.6)	1.35 (1.12)	2.12 (2.6)	50	1800	0.87

From the fuel properties in Table 3 several observations can be made. First of all, the lower calorific value from PG is more than eight times lower than diesel or natural gas. This means that the heat released per kg of fuel is also eight times lower, resulting in severe power derating of the engine. However, the air/fuel ratio`s from these fuels are also very different, resulting in mixture calorific values which do not differ much from each other. Based on only the mixture calorific value, derating of around 8% (compared to diesel) to 13% (compared to NG) can be expected when running an IC engine on this specific producer gas. Other critical properties that will influence the engine`s performance relating to the combustion process in the cylinder are the flame speed and product to reactant mole ratio. The flame speed is significantly higher for producer gas than for natural gas or diesel. This is mainly due to the presence of H_2, which has a flame velocity of 2.7 m/s. A higher flame velocity can, when the ignition timing is not adjusted, lead to knock or misfire. Also, the product to reactant mole ratio is lower for producer gas, which results in lower cylinder pressures, and thus less power output [5].

The composition of synthesis gas can vary a lot, as well as the composition of anode-off gas. To be able to predict the performance of an engine, it is important to understand how such a gaseous fuel behaves when combusted in an IC engine. Table 1 shows that changes in composition can change the peak flame temperature, flame speed, calorific value and thus the performance of an engine. First however, a comparison between anode-off gas and current studies with similar compositions will be made.

2-3 Current studies with similar compositions

For looking at similar compositions, it needs to be chosen with which composition of anode-off gas a comparison should be made. The composition of anode-off gas is given for different fuel utilization rates. A utilization rate of 50 or 60 % is relatively low. In reality, 75 or 85% should be obtainable so the current studies will be compared to these compositions.

For these compositions, a relatively high content of H_2 is present compared to synthesis gas studies. Also quite a substantial amount of CO_2 is present which none of the studies mentioned in Chapter 2 have. A close comparison can therefore not be made. However, when looking at the volume percentage of *combustible* species, it can be seen that the anode-off gas consist of roughly 40-60% of combustible products. This is the same for almost all the studies that use any kind of synthesis gas, apart from the studies that use combinations of pure H_2 and CO. Still, the percentage of combustible gasses does not say it all either, since different components have different properties.

It seems that making a comparison with existing studies can not be done because of the different composition of the gas. However, there are some trends that can be used. For example when looking at the power derating. In general synthesis powered engines provide roughly 60-70% of the power compared to diesel engines, and roughly 75-85% of the power compared to gas engines. The peak flame temperature of anode-off gas will be similar to that of producer gas, since both CO and H_2 have the same peak flame temperature, and therefore can be compared to the studies in [14], [15] and [16]. Also the amount of combustible gas is similar. Therefore similar deratings can be expected for anode-off gas, taking into account that proper tuning of the ignition timing and TC matching is carried out.

The relative high flame speed of H_2 in combination with the large amount of it present in anode-off gas will have an effect on the combustion process. In the dual-fuel mode it was shown that H_2 addition increased the overall efficiency. However, the attainment of the peak pressure lagged 8-15°. In general it was shown that the overall efficiency can be close to the same values as for conventional fuels. However, due to the lower calorific mixture value, a larger flow rate is necessary to reach acceptable performance levels. With the amount of CO and CO_2 present, relatively large amounts of CO_2 emissions can be expected.

Based on the composition of anode-off gas and comparing it to previous studies, it is expected that anode-off gas can be combusted in an IC engine. Adjustments will have to be made to support good combustion, like the flow to the engine. Also derating of the engine should be expected. Depending on the composition, it could be possible that either a compression ignition (CI) engine or a spark ignition (SI) engine will work better. To better understand this, it is important to know how synthesis gasses behave in different types of engines.

2-4 Synthesis gas in a CI engine

More strict regulations concerning the emissions of diesel engines has engine manufacturers looking for alternatives. One viable alternative for both the future scarcity of fossil fuels and emission regulations is the use of synthesis gas in diesel engines. It could reduce costs, reduce emissions (mainly NO_x and particulate matters) and increase engine performance. The only drawback is that synthesis gas has a high self-ignition temperature (above 500° C) and thus can not be ignited by compression ignition. It would need a pilot fuel like diesel to ignite [6]. As reported in earlier work by Boehman et al.[7], the use of H_2 and CO mixtures works better in lean burn conditions where combustion temperatures are moderated by air excess like in CI diesel engines.

Multiple studies have been done on dual fuel engines using syngas. In 2011 a study was performed by Sahoo et al. [8] on the second law analysis of a single cylinder DI CI engine fuelled with syngas under dual fuel mode and using diesel as a pilot fuel. They studied the effect of the H_2:CO ratio on the engine performance of a 5.2 kW diesel engine at different load levels. They reported that at higher loads, the syngas dual fuel operations are advantageous from the second law perspective compared to diesel fuel. With increasing load, the destroyed availability decreases due to higher combustion temperatures and pressure, and therefor the exergy efficiency increases.

In another study [9], the same authors did further research on the effect of the H_2:CO ratio in syngas, using the same 5.2 kW engine. They looked at brake thermal efficiency, pressure profile, maximum cylinder pressure, diesel substitution, exhaust temperature and emissions. The dual fuel engine with a H_2:CO ratio of 100:0 showed the highest brake thermal efficiency of 19.75% at 80% load as can be seen in Figure 1. This is lower than the 20.92% efficiency achieved using only diesel as fuel. At this ratio and load, they also found the maximum diesel replacement rate at 72.3%. At lower loads there is hardly any difference in the efficiencies of the different syngas compositions. At these loads, a small amount of pilot diesel fuel leads to poor ignition and combustion of lean air-gas mixture, which means that the H_2 content has a minor influence on increasing the thermal

efficiency. At higher loads, better combustion occurs, and an increase in H_2 content also increases the thermal efficiency due to a faster combustion rate [9].

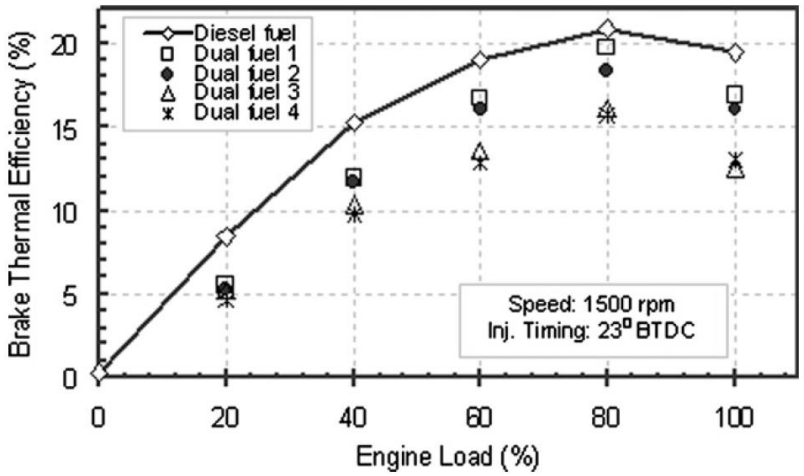

Figure 1: Variation of brake thermal efficiency with engine load, after Sahoo et al., 2011

The variation of the diesel replacement rate can be seen in Figure 2. Dual fuel 1 has the highest H_2 content, after which it decreases to 75%, 50% and 0%. Even with 100% CO, the diesel replacement rate is still 58.4%, occurring at 100% load, since CO has better combustion at higher temperatures. This shows that CO is a suitable gas as an alternative fuel in diesel engines.

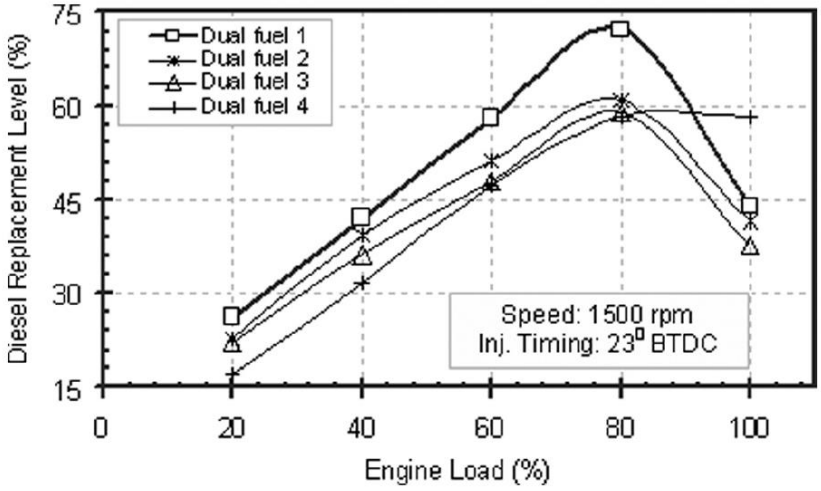

Figure 2: Variation of diesel replacement rate, after [4]

To produce the same power output as the diesel case, the low energy density syngas fuel needs more fuelling compared to using only diesel as fuel.

The attainment of the peak pressure is not the same for dual fuel operations as for diesel only operation. In dual fuel operation the peak lags 8 to 15 degrees of crank angle with the same ignition timing. In general, the peak cylinder pressure is lower for dual fuel operations. This is because of the shorter combustion duration and increased ignition delay for syngas dual fuel operations, which shift the overall combustion to the expansion stroke, resulting in a reduction of cylinder pressure.

However, as can be seen in Figure 3, the peak pressure for 100% H_2 is higher than for diesel mode. This is the result of the higher energy content of 100% H_2 and a more pronounced premixed combustion. Also at this ratio the highest in-cylinder temperatures are recorded. As a result, the exhaust gas temperatures and NO_x emissions are higher than for the other tested ratio`s including diesel only [4].

The fact that the performance of the engine is poor in part load conditions using syngas dual fuel, shows that the use of syngas is better for generator applications than for marine propulsion applications.

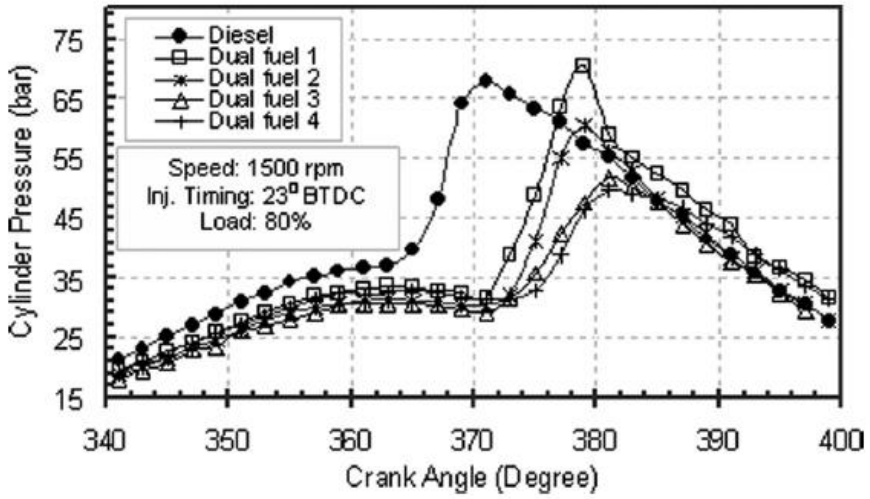

Figure 3: Variation of cylinder pressure with crank angle at 80% engine load, after [4]

In a study performed by Speath [10], a dual fuel mode of a CI engine was researched using both syngas and methane as the main fuel source. The composition of the syngas was 10% H_2, 25% CO, 4% CH_4, 12% CO and 49% N_2. It was found that for the same equivalence ratio (the actual fuel/air ratio to the stoichiometric fuel/air ratio), the brake torque and brake power produced by syngas is less than that for methane, and the energy input is less for methane than it is for syngas. Also, syngas operation produces lower thermal efficiencies and higher brake specific fuel consumption (bsfc) values for corresponding equivalence ratios in comparison to methane operation. Overall, methane shows better performance in dual fuel mode than syngas.

A complete replacement of diesel with syngas in CI engines is not possible because of the high self-ignition temperatures of syngas. It can however be used, and depending on the composition, it could reduce emissions as well as costs.

2-5 Synthesis gas in a SI engine

One of the major advantages of using synthesis gas in a SI engine is that the engine can run on 100% synthesis gas, since no pilot fuel is needed to ignite the mixture. A drawback of using a SI engine is the lower compression ratio (CR) compared to CI engines. A lower CR reduces the thermal efficiency, which means that less energy can be extracted from the same amount of air/fuel mixture. This will result in power derating of the engine compared to higher compression ratios.

Generally a lower CR is necessary to prevent engine knock when using a SI engine. This was thought to be the case as well with a SI engine running on synthesis gas. However, research by Sridhar et al. [11] shows that a compression ratio of 17:1 is possible without knocking when running an engine on producer gas. The presence of CO_2 and N_2 helps, since these inert gasses have a high anti-knock behaviour because they suppress the pre-flame reactions that are responsible for knocking.

Multiple studies and experiments have been done on running SI engines on synthesis gas. In 2010, a study was performed by Shah et al. [12] on the performance and emissions of a 5.5 kW spark-ignited engine driven generator on biomass based syngas. The composition of the syngas they used was 16.2-24.2% CO, 13-19.4% H_2, 1.2-6.4% CH_4, 9.3-13.8% CO_2 and the remaining N_2. They found that the efficiency of the engine was almost the same when running it on syngas (19.1%) compared to running it on gasoline (19.3%). The maximum electrical power output was lower for syngas (1392W) compared to gasoline (2451 W) due to the lower calorific value of the syngas. Emissions of NO_x and CO were significantly lower for syngas. However, the CO_2 emissions were much higher due to the presence of CO_2 in the syngas.

A study on a 6 cylinder 55 kW NG engine fuelled with producer gas was done by Shivapuji et al. [13]. They showed that parameters that are to be optimized for operating the engine on producer gas are the ignition timing for maximum brake torque (MBT) and the carburetion system. The ignition timing needs to be adjusted because of the higher flame speeds and the intake needs to be adjusted to accommodate the high fuel flow rates, since air and fuel are supplied in almost the same proportions. The average producer gas composition they used contained 16.04% CO, 16.92% H_2, 10.5% CO_2, 1.22% CH_4 and balance N_2. They found that with this composition the ignition timing needed to be advanced by 2 degrees from the original setting of 22 degrees before top dead center. With this setting, a peak load of 29 kW at 1500 rpm was found with a brake thermal efficiency of 23%.

The performance of a producer gas engine coupled with a 75 kWe generator was studied by Raman et al. [14]. The performance is compared with diesel and natural gas engines. The composition of the producer gas is 23% of H_2, 21% of CO, 0.9% of CH_4, 9% of CO_2 and 46% of N_2. According to the authors, the non-combustible gasses affect the engine's efficiency in two ways. First of all they reduce the energy density of the producer gas. Secondly, most of the heat generated during the combustion phase is absorbed by these non-combustible components and thus the adiabatic flame temperature is reduced. This results in a low expansion ratio of the fuel mixture, which reduced the efficiency of the engine. In the same study, the compression ratio of the engine is varied between 7:1 and 12:1. The highest efficiency (21%) was achieved at the highest compression ratio at 85% load. At this point, the efficiency is 12.5% lower than the same engine on natural gas.

The importance of the CR is becomes clearer when comparing the previous experiment of Raman et al. with the experiment of Gobbato et al. [15]. In their experiment, they run a 250 kW NG engine on producer gas, without increasing the CR. The ignition timing is advanced from 16° BTDC to 28° BTDC, and stoichiometric air/fuel ratios are used. The composition of the producer gas is 18% H_2, 20% CO, 1% CH_4, 12% CO_2, 49% N_2. The engine power derating exceeds 50% due to the significant reduction of the volumetric efficiency, which almost half of that for NG. The volumetric efficiency drops because PG takes up more volume than NG for the same energy content. It shows

that NG engines can run on producer gas, but adjustments need to be made in order to minimize power and efficiency losses.

The effect of right adjustments has been shown by Shivapuji et al. [16]. In their study they use 3 engines, originally designed as diesel engines, which are converted to NG engines and then run on producer gas. The nominal diesel ratings in kWe are 500, 250 and 90. The CR is reduced by 3.1, 5.5 and 6 units to make sure no engine knock occurs. In previous work by Dasappa [17] it was established that a unit change in the CR can reduce the engine peak power between 1-3%. This means that a thermodynamic derating of respectively 46.5, 41.2 and 16.2 kWe can be expected for the three engines because of a CR reduction. Also they calculated the expected derating due to the lower calorific value and then could calculate the expected power from the engines. During experiments however, they found that the power output from the engines was much less than the theoretical value, meaning there was another derating component, which was the highest of all. The only plausible reason for this is the constraint of the mass flow to the engine, which was verified by gas mass flow measurements on each engine. It showed that the extra derating component was due to the turbocharger mismatch under the new operating conditions. The pressure ratio over the compressor of the turbocharger is 1.5 for the 500 and 250 kW engines and 1.2 for the 90 kW engine, compared to 2.4 for the same engines using diesel as fuel. They identified that the power derating due to the turbocharger mismatch and the low mixture calorific value were non-thermodynamic in nature and thus had a potential for recovery. An overview of this is given in Figure 4.

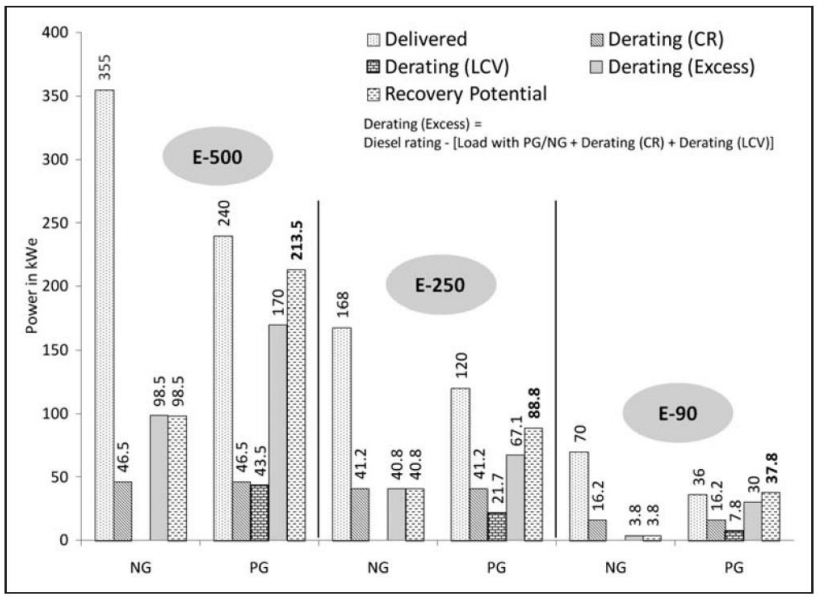

Figure 4: Power derating distribution comparison for three engines, after [16]

The recovery can be achieved in theory by increasing the gas mass flow to the engine. This would be possible by turbocharging matching. A more detailed study was done on the 90 kW engine. A zero-dimensional Vibe function-based model with knock prediction capabilities was used for engine simulation, predicting a knock limited peak load of 76 kWe, which is close to the 73.8 kWe prediction when full recovery is reached from the non-thermodynamic losses. Different turbochargers were investigated, of which the compressor maps are shown in Figure 5. Looking at the compressor map for TC-1, it can be seen that around 65% of the PG peak load, the operating

points are outside the operating range of the turbocharger. At 85% of the peak load the surge line of the turbocharger is crossed. It shows a clear mismatch. Turbocharger 4 has a much better match, which results in a peak load of 72.8 kWe, which is more than a 98% recovery rate of the non-thermodynamic losses.

Besides the turbocharger matching, they also looked at the nature of combustion at various inlet temperatures. It was found that knock started at inlet temperatures above 55° C, and knock was established at temperatures between 58 and 65° C. After this, heavy knock occurred. It shows that an aftercooler becomes an essential part of the engine when optimizing an engine for producer gas.

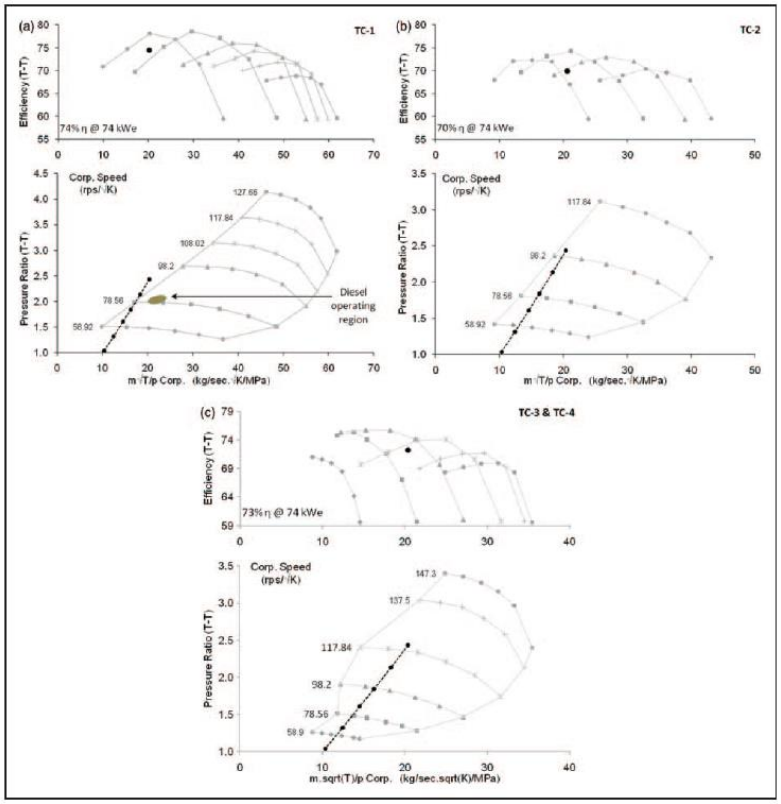

Figure 5: (a) Compressor map TC-1. (b) Compressor map TC-2. (c) Compressor map TC-3 and TC-4. After [16]

2-6 Engine power derating

Engine power derating has been briefly discussed in the previous chapter. Since it is important to know what to expect in terms of power derating when using anode-off gas, an overview will be given on different experiments with their corresponding gas composition and engine power derating. This overview is presented in Table 4. All experiment were done at stoichiometric conditions, or just on the lean side of this. Derating of the engine is given as a percentage of the original nominal power.

Table 4: Comparison of engine power derating

Authors	Fuel (Vol. %)	LCV mixture (MJ/kg)	Engine type	Derating
[18]	CO 52% H_2 44% N_2 4 %	15.3	Ricardo E6 single cylinder SI	30% compared to gasoline, 23% compared to NG
[12]	CO 16.2-24.2% H_2 13-19.4% CH_4 1.2-6.4% CO_2 9.3-13.8% N_2 remaining %	5.79	5.5 kW SI, NA single cylinder generator	43% compared to gasoline
[13]	CO 16.4% H_2 16.92% CO_2 10.5% CH_4 1.22% N_2 remaining %	4.2 MJ/m^3	Cummins, 55 kW SI, NA 6 cylinder	37% compared to NG
[3]	CO 21% H_2 23% CO_2 9% CH_4 0.9% N_2 46 %	5.6 MJ/m^3	6 cylinder 85 kW SI	12.4% compared to NG
[16]	CO 19% H_2 19% CO_2 9% CH_4 1.8% N_2 remaining %	5	6 cylinder, 5.9 L, 90 kWe (using diesel), 70 kWe (using NG), TA	60% compared to diesel without TC matching 19% compared to diesel with TC matching
[19]	Dual fuel diesel/PG CO 29% H_2 19% CO_2 8% CH_4 6% N_2 38 %	7.4	Diesel, single cylinder 4 kW NA	15% compared to diesel at 74% diesel replacement
[15]	CO 20% H_2 18% CO_2 12% CH_4 1% N_2 49 %	4.3	12 cylinder NG, SI, TC 250 kW	54% compared to NG

From Table 4 it is clear that engine power derating varies a lot, depending on different factors. First of all the composition of the gas determines how much energy is available for energy conversion. Secondly, the type of engine is important. A dual fuel diesel engine might have less power derating

compared to a 100% synthesis gas fuelled SI engine. Also, there seems to be a difference in naturally aspirating engines and turbocharged engines. Turbocharged engines can have a large power derating when fuelled with synthesis gas, but correct turbocharger matching can recover a lot of power. Besides this, ignition timing adjustments and CR changes can be done to further improve the performance of an engine running on synthesis gas.

2-7 Emissions

Even though emissions is not a main point of interest in this thesis, the general trend of emissions when using a synthesis gas will be provided here as found in the literature. The type and amount of emissions will depend on different factors, but one of the main factors is the type of fuel. For example, when there is no sulphur present in the fuel, there will be no formation of sulphur oxides.

In 2006, Mustafi et al. [18] found that their Ricardo E6 single cylinder SI engine produced very low THC emissions while running on a synthesis gas (0-20) compared to gasoline (90-225) and natural gas (20-106). Their synthesis gas consisted of 52% CO, 44% H_2 and 4%N_2. However, the CO_2 concentration was the highest for the synthesis gas, which is caused by the high amount of CO in the gas. NO_x emissions were found to be much higher compared to the other fuels, which was said to be due to the higher combustion temperatures and relatively short combustion.

In a study by Shah et al. [12] the increase of CO_2 emissions, when running on syngas compared to gasoline, was said to be because of the presence of CO_2 in the syngas, and the conversion of CO to CO_2 upon combustion. This agrees with the former study of Mustafi et al. However, the NO_x emissions were found to be 54-84% for syngas compared to gasoline. This does not agree with the previous findings. This difference can be explained when looking at the composition. The syngas compositions used by Shah et al. was 16.2-24.2% CO, 13-19.4% H_2, 1.2-6.4% CH_4, 9.3-13.8% CO_2 and the remaining N_2. The high content of N_2 causes the composition to have a lower calorific value than the composition as used by Mustafi et al. Due to the lower calorific value, the peak temperature in the cylinder will be lower. NO_x are formed from the oxygen and nitrogen at high temperatures in a reaction separate from combustion by Zeldovich mechanism [20]. Thus the higher N_2 content in the syngas results in a lower calorific value, which results in a lower peak temperature, which results in less NO_x emissions. This already shows the big influence of composition on the emissions.

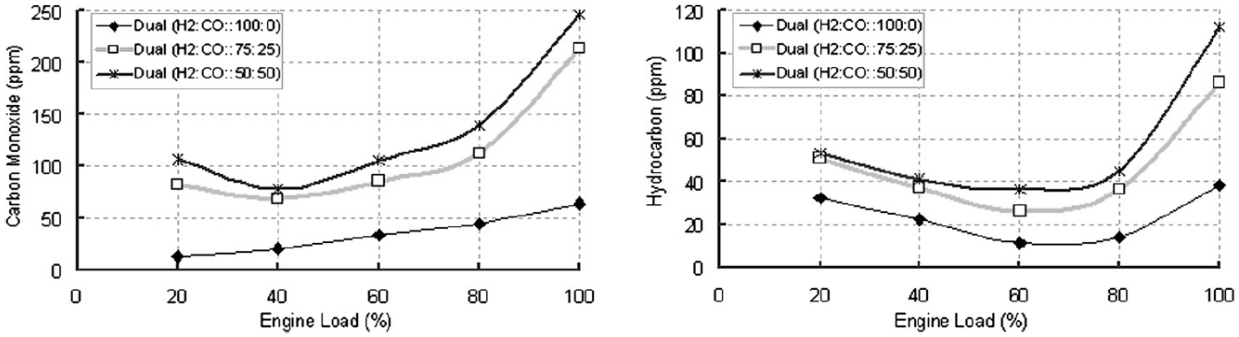

Figure 6: Left: variation of carbon monoxide with load. Right: variation of hydrocarbon with load. After [9].

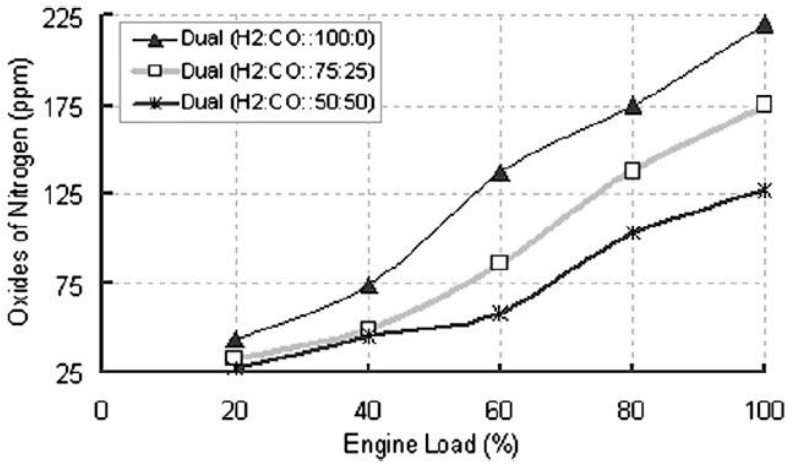

Figure 7: Variation of nitrogen oxides with load. After [9].

A similar result as was found by Mustafi et al. was also found by Sahoo [4] as mentioned in chapter 2.2, where it was shown that the higher content of H_2 resulted in higher temperatures, and therefore higher NO_x emissions, as can be seen in Figure 7. They also showed that the increase in CO content in the syngas results in an increase in CO and HC emissions in the exhaust, as can be seen in Figure 6. At the same time, a similar result to that of Shah et al. was found by Gobbato et al. [15], who also saw a decrease of NO_x emissions, this time compared to NG.

It can be concluded that the composition of synthesis gas has a big influence on the emissions. Emission reduction can definitely be achieved by using synthesis gas over a conventional fuel. Even addition of synthesis gas to a conventional fuel can already reduce emissions. However, a trade-off might have to be made between emissions and engine performance.

2-8 Modelling combustion

Computer models can be used to provide information on the performance of an engine. With the use of models, different configurations of an engine can be analysed without having to physically build different engines. When using engine models to assess the performance of an engine, it is important to know how close to reality (or how far off) the model predicts the performance. There

are different methods that can be used to model an engine, and in particular combustion. The main methods as described by [20], [21] and [22] are the following:

- CFD
- Phenomenological/multizone
- Filling and emptying
- Mean value modelling
- Transfer function

The Computational Fluid Dynamic (CFD) models provide very detailed information on the processes in the cylinder of an engine. The volume of the cylinder is divided in many different volumes or elements. For every timestep the basic equations between such volumes or elements are then solved. Different studies on synthesis gas using CFD have been done. Costa et al. [22] use a 3D CFD model to analyse the dual-fuel operation of a CI engine fuelled with diesel fuel and increasing amounts of syngas. Gamino et al. [23] use a 2D CFD model to simulate the syngas combustion process in a multi-spark engine. The same kind of model was used by Zang et al. [24], who studied partially premixed conditions. CFD models can give accurate results but can require high computational time [20], [25], [27].

In the phenomenological or multizone models, the combustion chamber is divided into a smaller number of control volumes, reducing the computational time. The main difference with CFD is that the multizone models do without an explicit solution of the turbulent three dimensional flow field [28].

In the Filling and Emptying (FE) method, the control volumes are various subsystems of the engine, for example the combustion chamber, intake and exhaust pipes, and the compressor. The laws of conservation of mass and energy are considered, but not the law of conservation of impulse. Since no flow fields are considered, this type of model is sometimes also called a 0-D thermodynamic model. Time steps are taken in the order of magnitude of a crank angle, therefore the model can also be referred to as crank angle model [20], [28], [29].

Mean Value (MV) models have the same origin as the filling and emptying method. The difference is that the time step is in the order of one revolution instead of one crank angle. Because of this, the discrete in-cylinder processes that take place within one revolution, have to be replaced by mean values [20]. This makes the mean value models simpler and faster than the filling and emptying method, but at the cost of accuracy. They are good models when only the overall engine parameters such as maximum cylinder pressure, manifold temperatures and pressures and turbocharger speed are of interest. This could be the case if the engine is to be incorporated in a larger system, for example when the complete drive chain of a ship has to be modelled [30], [31].

Examples of a filling and emptying model and a mean value model are the Diesel B (MV) and the Diesel C (FE) models, developed at the Delft University of Technology [23], [33]. The Diesel B model is a mean value first principal model which uses a revolution timescale instead of the crank angle timescale. This reduces the computational time, but it means that analytical models have to be developed which are solutions to the original differential equations of the crank angle model under certain specific conditions. A block diagram of the MVFP Diesel model is given in Figure 8. The primary input are fuel flow and engine speed, the secondary input is the ambient conditions.

The gas exchange model is fed by the air intake system, shown in blue. The air cover (AC), inlet receiver (IR) and outlet receiver (OR) are control volume elements. In here, the instantaneous mass is calculated by integrating the net mass flow while integrating the net energy flow associated with the net mass flow results in the instantaneous temperature. With these two, and using the gas law, the instantaneous pressure can be calculated. The control volumes are connected via resistances. In such an element, the mass flow is calculated as a function of pressure difference using the momentum equation. The processes in the cylinder are divided into discrete processes, with the combustion processes based on the Seiliger cycle [22], [27] and [34]. This can be seen in Figure 9.

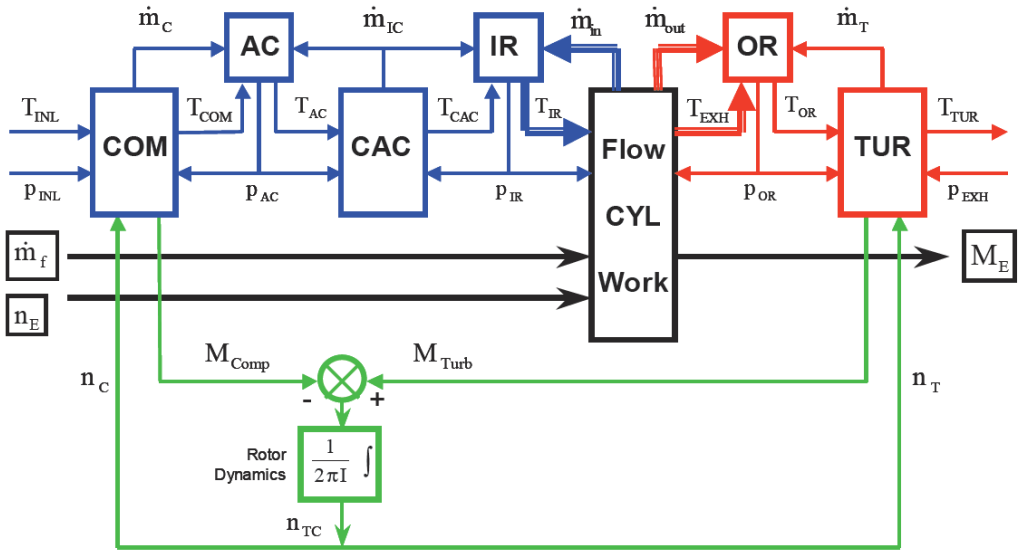

Figure 8: Block diagram of MVFP Diesel engine model. After [22]

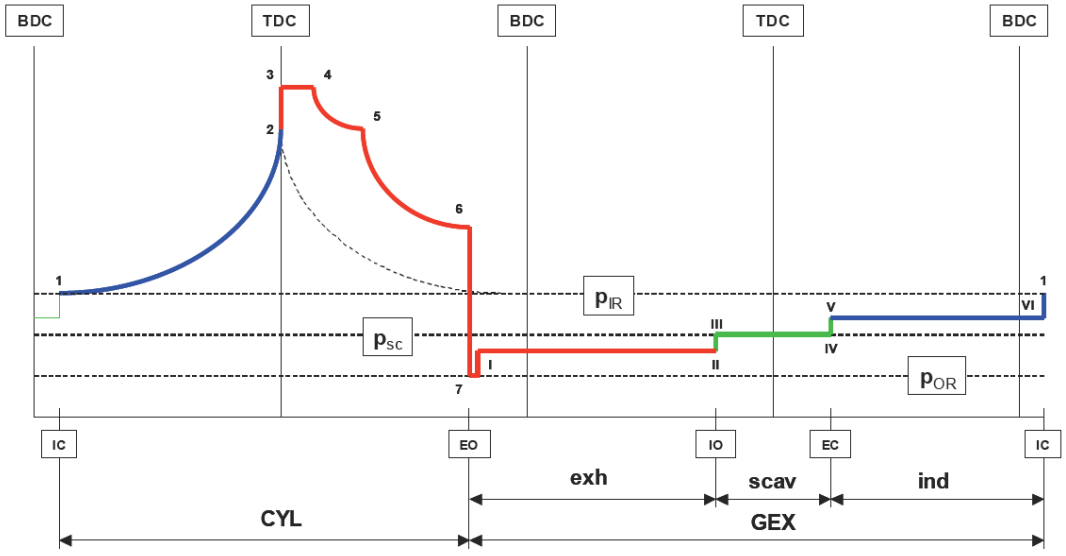

Figure 9: Conceptual model cylinder process 4-stroke turbocharged Diesel engine. After [22].

The Diesel C model simulates the in-cylinder processes from the moment the inlet closes (IC) until the moment the exhaust valve opens (EO). A block diagram of this in-cylinder model is given in Figure 10. The output of the model is the Temperature, which results from integrating the first law of thermodynamics. The volume is calculated using the crank angle and the cylinder geometry. The in-cylinder pressure is calculated using the gas law. In this model, the heat loss to the wall is modelled using Woschni`s model [35]. The heat release model uses a double Vibe function to make the model more suitable for real combustion processes and to make a distinction between the premix and the diffusive combustion stages.

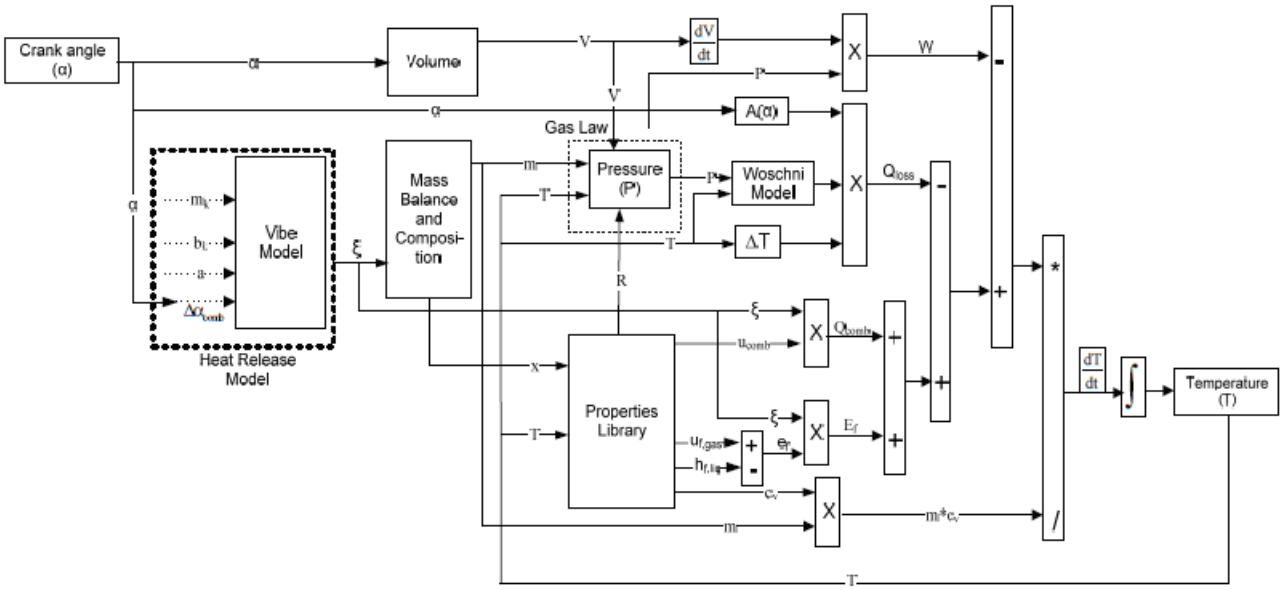

Figure 10: Block diagram of in-cylinder process model. After [23].

A distinction can be made on how the cylinder volume is treated. When the cylinder volume is treated as one zone, it is called a single zone model. In this case, parameters are spatial averages which represent the state within the cylinder. There is no difference made between liquid fuel, unburned mixture and incompletely oxidized fuel. This approach simplifies the model, but may not be sufficient when liquid fuel is present or when formation of for example NO_x need to be studied.

A two-zone model has been well described by Merker et al. [36]. They divide the cylinder volume in an unburned mixture zone and an incompletely oxidized fuel zone. The zones are separated by a flame front, which has no mass and is infinitesimal thin. A similar model was used by Linden [37] in an attempt to model the NO-emissions in a diesel engine. In another study performed by Lopez [38], the in-cylinder process for diesel engines was modelled using a three-zone model. Here, also the liquid fuel was separately modelled. However, since the evaporation rate followed closely the injection rate, it was proposed to continue with a two-zone model where no liquid fuel exists.

Most models that use more than 1 zone for the cylinder volume seem to be focussed on diesel engines, and in particular the formation of NO_x. Since in this thesis the performance of an engine using anode-off gas will be investigated, which will enter the system in a premixed condition, it seems that a single zone model should be sufficient.

Transfer function models can be used if only engine output is needed. In this case the engine is modelled as a simple second or higher order system with some basic dynamical aspects [20].

2-9 Modelling an engine on synthesis gas

The crank angle models and the mean value models are probably the most common modelling types used in engine performance analysis. Most of the studies in the maritime sector using these models are focussed on the performance of Diesel engines [39], [40], [28], [27]. The increase in the use of gas engines, due to more strict emission regulations and the future scarcity of petroleum fuels, has led to more research into gas engine modelling as well. For example, Georgescu [34] used both the Diesel B and the Diesel C model, and made modifications to investigate the transient behaviour of gas engines of the dual fuel type.

When looking more into the field of synthesis powered engines, modelling has also been done. In 2006, Sridhar et al. [41] used a zero-dimensional, two-zone model to predict the performance of a gas engine running on producer gas. The model used a wrinkled flame theory for the flame propagation. The model was validated using experimentally acquired p-α curves for a range of CRs and ignition timing. Turbulence parameters were extracted from a previously conducted CFD study and used as model input. The model was then used for a predictive performance evaluation. It proved to make reasonably accurate predictions at advanced ignition settings (above 17° BTC). At less ignition settings the model proved not yet very accurate. Another zero-dimensional model was built by Rakopoulos and Michos [42]. However, they used a multizone cylinder model. This was done to accurately predict the in-cylinder NO emissions at various engine loads for a syngas fuelled, SI gas engine. The model performed better in terms of NO emission prediction than a single zone model, but there is still an overprediction of around 50%.

Shivapuji and Dasappa [43] use a zero-dimensional model to predict the performance of a 6-cylinder gas engine under naturally aspirating and turbocharged conditions, fuelled with producer gas. Experimental heat release profiles are used to estimate the Vibe parameters used in the model. They saw from experiments that the heat release profile was significantly different for producer gas compared to gasoline. An overview of this is shown in Figure 11.

.

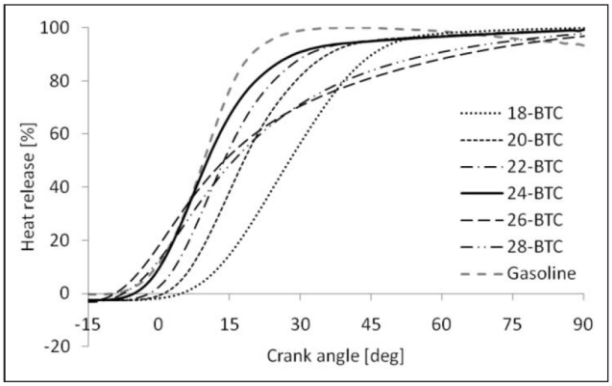

Figure 11: Heat release profiles at various ignition angles compared to gasoline. After [43].

The figure shows that for the MBT timing at 24°, the PG heat release pattern follows the gasoline heat release pattern in the first part, but is significantly different in the second part. The same pattern is seen for different percentages of the peak load, both for NA and TC modes. It seems that the combustion of producer gas is sluggish in the second half of the combustion, leading to an overall increase in the combustion duration. Also, at advanced ignition settings, the heat release pattern does not follow the typical S shape. This slow and extended combustion duration resulted in a significant power drop, 44% for 4° advanced ignition timing from MBT. This shows the importance of finding the right MBT timing with respect to engine performance. The enhancement of the combustion duration was finally attributed to the cooling of the mixture near the wall, leading to flame de-speeding, and increased combustion duration. This big difference is also seen in Figure 12, when looking at the pressure trace from their experiments, compared with the simulation results, where they first use standard Vibe coefficients (a=2, m=5) for the heat release model. This big difference shows the need for fuel specific Vibe coefficients for producer gas.

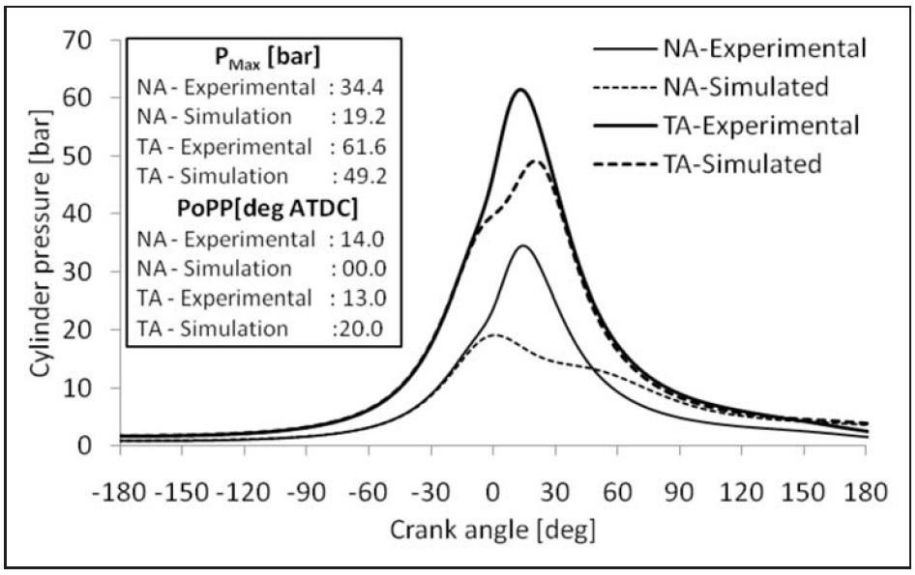

Figure 12: Comparing 0-D simulation with experimental pressure trace using standard Vibe coefficients. After [43].

The Vibe efficiency factor *a* is estimated using detailed measurements on the engine exhaust composition and temperature. Based on the exhaust gas temperature and the mass fraction of CO in the exhaust gasses, the combustion inefficiencies are estimated using:

Equation 2-1

$$1 - \eta_c = \frac{\sum_i X_i Q_{HV_i}}{\frac{F}{A} Q_{HV_f}}$$

The value for *a* was found to be 2.4. The shape factor was determined using the least square method and is estimated at 0.7 for both NA and TC operations.

The fuel specific Vibe coefficients were used in a new simulation and now the results showed a near complete match with the experimental data. However, it is easy to make a simulation fit the experimental data, but it does not mean yet that these fuel specific Vibe coefficients are correct.

They also performed a test with a 3-cylinder diesel engine converted to SI operation, running on producer gas. The results for the pressure trace for both the experimental data and the simulation are shown in Figure 13, for 2 compression ratios. The simulated data seems to have a good fit with the experimental data for a CR of 11.5. However, for a CR of 13.5, the position of the peak pressure is slightly advanced and the magnitude is slightly lower. A reason for this could be that a higher compression ratio increases the in-cylinder temperatures, which influences the flame speed and thus combustion duration. Adjusting the end of combustion angle results in a near complete fit.

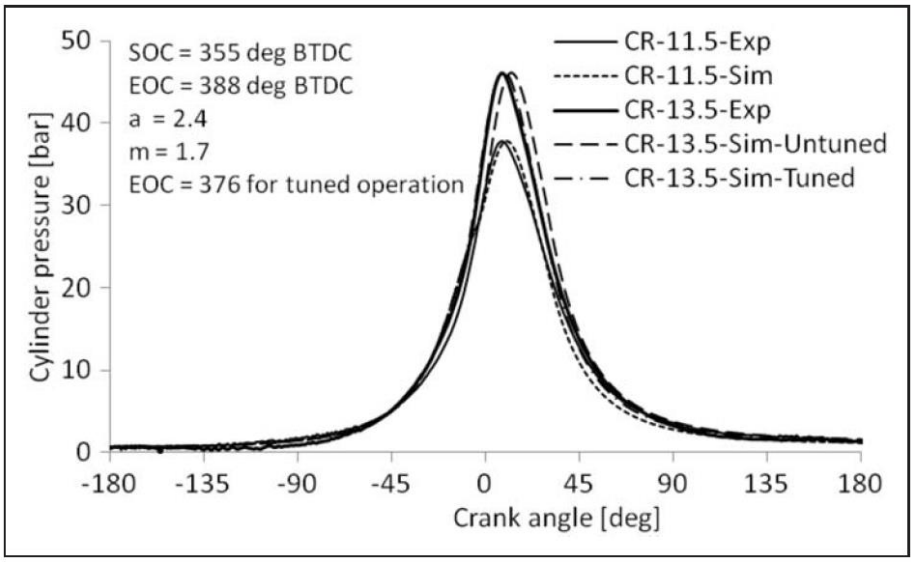

Figure 13: Comparison of experimental and simulated pressure traces. After [43].

The same authors used the same model in 2014 [16], but now they included knock prediction capabilities. They developed a chemical kinetics module composed of 53 species in a reaction mechanism involving 325 reactions, and integrated this with the Vibe function-based module to enable knock prediction. The idea is that at each crank angle, the change in enthalpy, pressure, and temperature of the mixture due to the change in specie concentration, is evaluated by solving for all the specie concentration change rate equations. Incorporation of chemical reaction kinetics ensures sudden release of all the energy associated with the un-burned mixture, representing knock, if the mixture thermodynamic conditions are such that the induction time (time for auto-ignition) at any particular time is lower than the corresponding burnout time [44].

2-10 Choosing the engine type and modelling method

Now that more is known from literature on different gases and modelling methods, several sub questions as phrased in the introduction can be answered. In the current chapter it has already been seen how anode-off gas compares to similar gases, and what current studies have been done into similar gases. Also power deratings and efficiencies have been briefly discussed as well as emissions. More on derating and efficiency will follow in later chapters. First the engine type and modelling method will be chosen.

2-10-1 SI versus CI

In Chapter 2 combustion of synthesis gas in both CI and SI engines has been discussed. In both cases the engine could run on synthesis gas, although the CI engine has to operate in dual fuel mode because of the high auto-ignition temperatures of synthesis gas. In that case, a maximum diesel replacement of around 73% can be reached. This is however with a 100% H_2, which is not available as anode-off gas. That means that a lower diesel replacement ratio would be achieved. The engine should in this case run on high loads because of the poor combustion characteristics at low loads.

When using synthesis gas in SI engines, the engine can run on 100% synthesis fuel. There can be quite a significant drop in engine performance, definitely when it is a naturally aspirating engine. When a turbocharger is properly matched, almost all lost power due to the non-thermodynamic losses (lower LCV and CR) can be regained. Ignition timing and carburetion system adjustments can further improve the performance of the engine.

Depending on the fuel utilization, the composition of the anode-off gas changes quite drastically. It is therefor not possible to select a certain type of engine based on the composition of the anode-off gas.

CI engines have a higher compression ratio than SI engines. It has been shown in Chapter 2 that a CR of 17:1 was possible when running an engine on producer gas, without knock occurrence. A higher compression ratio is favourable in terms of efficiency and power, due to the higher volumetric efficiency. This is in favour of CI engines.

However, in the GasDrive project, natural gas is used for power generation. When using a dual fuel engine to combust the anode-off gas with the given H_2 volume percentages, less than 70% of the diesel can be replaced. This means that still quite a sufficient amount of diesel needs to be taken onboard. In the search for less emissions and alternative fuels, this does not fit in. Also, technology is available to combust gas compositions like the anode-off gas in SI engines, and engine adjustments have proven to further improve the performance of such engines running on these type of gasses. Next to that, most research done on synthesis gas engines have been done using SI engines, so most available literature is on SI engines. Because of these reasons, an SI engine will be chosen to continue the research into the combustion of anode-off gas.

2-10-2 Engine adjustments

From previous studies mentioned in Chapter 2, it is clear engine adjustments need to be made. When modelling, it is easy to adjust certain components. However, when a real engine is being used, this is more difficult. From the literature it seems that the following needs to be done:

- Convert a CI engine to SI operation, to be able to obtain a higher compression ratio. Most favourable is if the CR is adjustable
- Ignition timing needs to be adjusted, due to higher flame speeds and different combustion duration
- Flow toward the engine needs to be increased, to compensate for the lower calorific value

2-10-3 Engine modelling method

To be able to choose a good modelling method, it needs to be clear what exactly needs to be investigated. In this case, the performance of an IC combustion engine running on different compositions of anode-off gas is being researched. The goal is to determine if it can be used for power generation onboard a vessel. This will only be done theoretically and not experimentally.

Since no experiments will be done, there will be no experimental data to validate a model. Since the model does need to be verified, it will first be used on experimental data from Shivapuji et al. [44], [43], [16] and [13]. Many experimental data sets are available for different engines, of which the most data is available for a 70 kWe NG engine. The model will be built with the input from the experiments on this engine, after which it will be verified for the same composition of synthesis gas in a different engine. Once the model is verified, it will be used to analyse the combustion of anode-off gas.

Differences in composition can have a big impact on the combustion profile in the cylinder, and therefore how the engine performs. As seen before, finetuning of different engine parameters is needed to get an acceptable performance. Therefore the in-cylinder zero-dimensional model (Diesel C model) will be used, with fuel-specific Vibe parameters for the heat release model. Also in all the literature found on modelling combustion of synthesis gas, a zero-dimensional model has been used, showing it is the obvious choice. Since emissions are out of the scope of this thesis, a single zone model will be used. CFD models will be to computational expensive and do not give the wanted performance parameters. A mean value model would not give the wanted level of accuracy.

2-10-4 Input parameters for engine model

The Diesel C model which will be used, returns the in-cylinder temperature as output after integration of the first law of thermodynamics, which is then used again as input. The simulation runs from the moment the inlet valve closes, until the moment the exhaust valve opens. Different input parameters are needed, which include the trapped pressure and temperature, type of fuel with its properties, type and size of the engine, a heat release model and a heat loss model. All of these inputs individually can change the outcome of the simulation and care needs to be taken that the right input parameters are used. Because of the significant differences between synthesis gasses compared to conventional fuels, some of these input parameters need to be changed. More on the input parameters and how they change when switching to a synthesis gas, will be explained in Chapter 3.

2-11 Summary

The main components of the anode-off gas are H_2, CO, CO_2 and H_2O. A similar gas to anode-off gas is synthesis gas, which has been used in both CI engines and in SI engines. CI engines cannot run on 100% synthesis fuel because of the high auto-ignition temperatures of the gas. Therefor a pilot fuel, mostly diesel, will be used and the engine will run as a dual fuel engine. The composition of the gas determines the calorific value, which says something about the amount of energy available for energy conversion. In dual fuel mode in a CI engine, the best performance is achieved when more H_2 is present in the gas. The pressure peak, ignition timing and ignition delay will

change, mostly resulting in loss of power and efficiency. Poor engine performance occurs in dual fuel mode at low loads because of poor combustion properties. In SI engines, synthesis gas can be used as the only fuel. The lower CR of SI engines compared to CI engines is a drawback concerning the engine performance on synthesis gas, since the gas has a low calorific value. However, higher CR's have proven to be possible, resulting in higher performances. For even better performances, the ignition timing and carburetion system should be adjusted, and in case of turbocharging, the turbocharger should be matched to the new operating conditions when running on synthesis gas.

Depending on the wanted simulation time and accuracy, different engine simulation models can be chosen. These are in order of decreasing complexity and accuracy:

- CFD
- Phenomenological/multizone
- Filling and emptying
- Mean value modelling
- Transfer function

Mostly used for engine performance analysis are the Filling and Emptying models and the Mean Value models. In research into combustion of synthesis gas in SI engines, most studies use a zero-dimensional model. Depending on the interest of research, a single, double or multizone cylinder volume is chosen.

For this research, an SI engine will be modelled because then no diesel is needed and most research that can be found, has been done on SI engines. When modeling the engine, ignition timing and fuel flow to the cylinder will for sure have to be altered compared to CI simulation. To model the combustion, an in-cylinder model will be used.

Before continuing the research part of this thesis, the research methodology will be further discussed and the modeling of the used engine will be further elaborated upon in the next chapter. After that, the model is matched to data from literature. Before being able to simulate anode-off gas using the model, more needs to be known on how anode-off gas combustion will behave compared to the gas used to match the model, which is first researched. Lastly the model is used to simulate anode-off gas combustion.

3 Research methodology and engine modeling

In the previous chapter a literature study was conducted. The properties of anode-off gas turned out to be similar to the properties of syngas and therefore more information has been given on different studies with syngases. Also more information has been given on different modeling methods. As it seems, an in-cylinder model is the best modeling method to use in the current study, and is therefore adopted. To be completely independent of fossil fuels, an SI engine model is used. The global methodology of this research has shortly been discussed in chapter 1. For more clarification throughout the next chapters, the research methodology is explained in more detail in this chapter. After this explanation, more information is given on the engine model and how this model has been changed in order to use it for the combustion of anode-off gas.

3-1 Research methodology

The goal of this thesis is to research the performance of an IC engine on different compositions of anode-off gas, and to see if it can be used for power generation onboard ships. The idea is to build an engine model with which the combustion of anode-off gas can be simulated. Because no research has been done into the combustion of anode-off gas, first a literature study has been conducted to get more insight into what can be expected when combusting anode-off gas, and what the best way of modelling is for this study. The following has become clear from the literature study:

- A similar gas to anode-off gas is syngas, for which several experimental and numerical studies have been done by different researchers.
- Syngas needs a pilot fuel when used in a CI engine. Anode-off gas is, due to similar properties, expected to need the same. To be able to use anode-off gas as a sole fuel, a SI engine should be modelled.
- To research the combustion of anode-off gas and say more about the engine performance, in-cylinder changes during one revolution need to be known. Therefore an in-cylinder model will be used.

With the above points clear, the next steps are taken. First of all an engine model needs to be further developed. An engine model is available at the Delft University. However, this engine model is based on a diesel engine while this thesis will use a SI engine. Building an entire new model takes a lot of time. Therefore the existing engine model will be modified to work as a SI engine in which anode-off gas combustion can be simulated. The necessary steps in changing the engine model will be further discussed later in this chapter.

With the engine model modified, it still needs to be verified. Data from literature will be used for this. Several studies have been found on combustion of syngas, which is similar to anode-off gas. In some of these studies, experimental results are given. These results will be used to verify the engine model. Most information is available from a study conducted by Annand Shivapuji [43]. Detailed pressure-crank angle curves, as well as other data from his study will be compared with the output from the engine model, using the same input as in his experiments, like trapped temperature, pressure, and composition of fuel. Using the same input, the output should also be similar.

When the engine model is working properly, the base model to start looking at anode-off gas combustion is ready. However, combustion of anode-off gas will not be entirely similar to syngas. One of the main differences between anode-off gas and syngas is the hydrogen content, which is higher for anode-off gas. Since hydrogen has a high flame speed, the increase in hydrogen is expected to increase the flame speed as well. A higher flame speed would mean that the fuel burns faster, which evidently can shorten the combustion duration. Since combustion duration is one of the inputs for the engine model, it needs to be known how the combustion duration will change with changing the composition. This is further researched in chapter 5. In this chapter, a relation is sought between the flame speed and the combustion duration. As will be shown, it is very difficult to find a clear link between the flame speed and combustion duration. However, a method is found which does link these two. More on this is explained in chapter 5.

With the combustion duration for anode-off gas as input for the engine model, the model can be used for simulating the combustion of anode-off gas. To be able to compare this to other data, the same engine and conditions at the moment of inlet valve closing are chosen as used by A. Shivapuji in his experiments. This way, the results can be compared to existing results. These results will be further analysed and conclusions and recommendations will be given.

3-2 Introduction to the Diesel C model

The Diesel C model has been briefly discussed in chapter 2-8. For the purpose of better understanding, the model will be described more comprehensively. The main workings and ideas behind the model will be explained further, like the thermodynamics of the model and the way the heat release profile is modelled. Also the heat loss will be shortly discussed. Once this is more clear, the changes needed to simulate anode-off gas combustion will be explained in chapter 3-3.

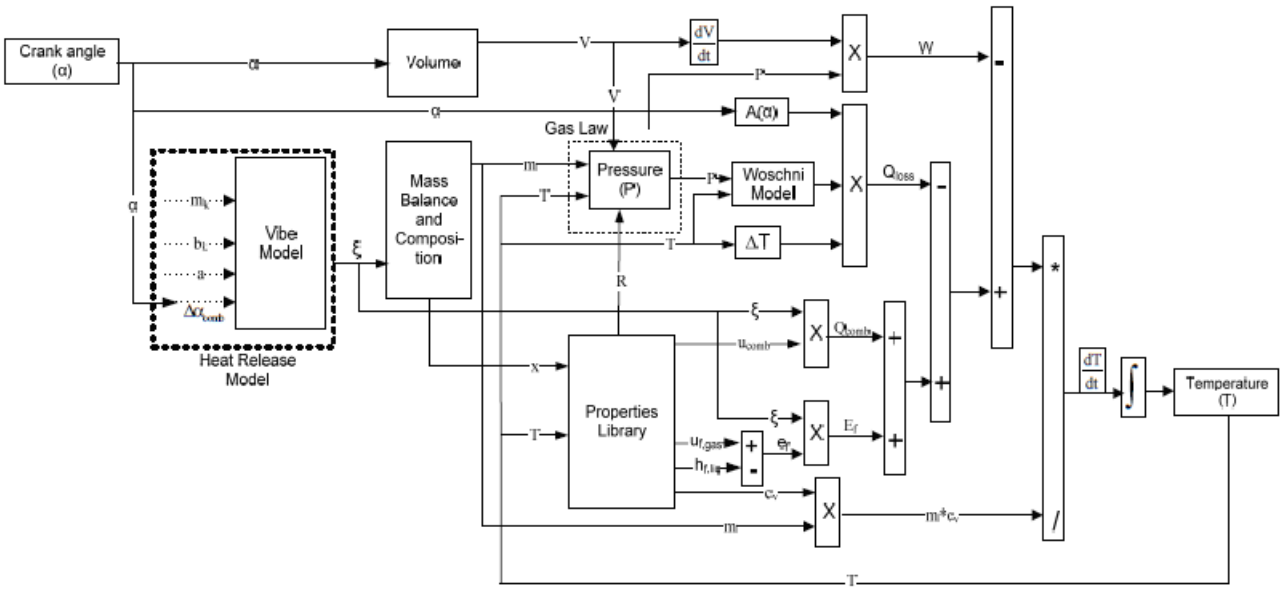

Figure 14: Block diagram of in-cylinder process model. After [23].

3-2-1 1st law thermodynamics

Since energy cannot be created or destroyed, but is rather transferred, the first law of thermodynamics is used in the engine model. Figure 14 shows a block diagram of the in-cylinder process model. This model simulates the in-cylinder processes from the moment the inlet valve closes until the moment the exhaust valve opens. One of the outputs of the model is the in-cylinder temperature which follows from integration of the first law of thermodynamics:

Equation 3-1

$$\frac{dT}{dt} = \frac{\dot{Q}_{comb} - \dot{Q}_{loss} - p \cdot \frac{dV}{dt} + \dot{E}_f}{m \cdot c_v}$$

In which:

$\dot{Q}_{comb}$ = heat release of the combustion
$\dot{Q}_{loss}$ = heat loss
$p \cdot \frac{dV}{dt}$ = (when integrated) work of the system
$\dot{E}_f$ = energy of fuel

This temperature is fed back into the model to calculate for example the pressure and work. The volume of the cylinder is calculated using the geometry of the engine and the crank angle. The volume is needed in the gas law, together with the temperature and the mass, to calculate the pressure. The volume and pressure together can then be used to calculate the work done by the engine.

3-2-2 Heat of combustion

The heat of combustion is calculated using the Combustion Reaction Rate (CRR or ζ) and the effective heat value for the closed system u_{comb}. During combustion of the mixture in the cylinder, the composition will change and therefore the properties of the mixture will change. These are calculated in the properties library using the air mass fraction of the mixture and then used to calculate the heat of combustion:

Equation 3-2

$$\dot{Q}_{comb} = CRR \cdot u_{comb}$$

The way the air mass fraction is calculated will be different from the conventional Diesel model as will be explained later.

3-2-3 Vibe coefficients

To describe the heat release profile, the Russian scientist Wiebe proposed a correlation for the cumulative heat release profile. This correlation is also known as the Wiebe or Vibe function. It provides a curve fit for the cumulative heat release profile in the form of:

Equation 3-3

$$X = 1 - e^{-a \cdot \tau^{m+1}}$$

in which X stands for the normalized combustion progression. The coefficient *a* is related to the fuel conversion efficiency according to:

Equation 3-4

$$\eta_c = \frac{Q_{released}}{Q_{supplied}} = 1 - e^{-a}$$

The coefficient *m* is the shape factor, which allows for tuning the S profile of the cumulative heat release, to minimize the difference with the experimentally derived heat release profile. The influence of changing *m* can be seen in Figure 15. With changing this parameter, almost any shape of the heat release can be modelled.

When a non-dimensional rate of combustion is introduced according to:

Equation 3-5

$$Z = \frac{dX}{dt}$$

In which:

τ = non-dimensional time, defined as:

Equation 3-6

$$\tau = \frac{t - t_0}{\Delta t_{comb}}$$

in which:

$t\text{-}t_0$ = time since beginning combustion
Δt_{comb} = total combustion time

Then a link with the reaction rate can be made according to:

Equation 3-7

$$\zeta = Z \cdot \frac{m_{f,0}^{comb}}{\Delta t_{comb}}$$

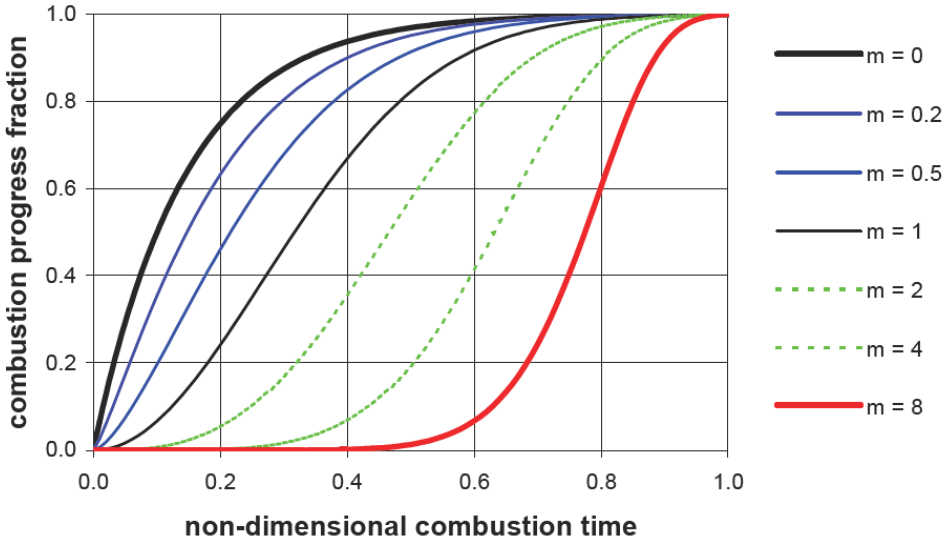

Figure 15: Influence of shape factor *m*, after [44]

3-2-4 Heat loss

The heat loss ($\dot{Q}_{loss}$) occurs due to the temperature difference between the hot gas and the cooler cylinder wall, cover and crown. This heat loss should be taken into consideration. The heat loss is calculated using:

Equation 3-8

$$\dot{Q}_{loss} = \sum_{i=1}^{3} \{\alpha_{g \to w} \cdot (T - T_{wall,i}) \cdot A_{wall,i}\}$$

In which:

i=1, cylinder wall
i=2, cylinder cover
i=3, piston crown
α=heat transfer coefficient
A_{wall}= Area cylinder wall

The heat transfer coefficient is usually determined with the Woschni method. As will become clear in chapter 3-3, this is not always the best option to calculate the heat transfer coefficient.

The final output of the model is the temperature. This temperature however is used again to calculate several other parameters. This means that the model needs to start from somewhere, and initial conditions need to be given. These initial conditions are the conditions when the inlet valve closes.

3-3 Modifying the model

Before using a synthesis gas as fuel in the model, the model needs to be modified. Not only will a synthesis gas be used instead of Diesel, but also a SI engine will be modelled instead of a CI engine. This causes several changes which will be discussed below.

3-3-1 Mass balance

The mass balance is different from the Diesel mass balance since the trapped mass is the total mass because air and synthesis gas come into the cylinder in a premixed condition. This means that there is no fuel injection later on.

The total mass trapped in the cylinder at the moment the inlet valve closes is calculated using the gas law

Equation 3-9

$$m_t = \frac{p_1 V_1}{R_1 T_1}$$

in which the mass is the only unknown and can therefore be calculated The other parameters are given or calculated based on fuel composition or engine geometry. The mass consists of stoichiometric gas from the previous cycle (m_{sg}), air (m_a) and fuel (m_f). A mass fraction of stoichiometric gas from the previous cycle is assumed (x_{sg}). This means that trapped air mass fraction and trapped fuel mass fraction can be calculated through

Equation 3-10

$$x_a = (1 - x_{sg}) - x_f$$

in which the mass fractions are defined as:

Equation 3-11

$$x_a = \frac{m_a}{m_t}, \quad x_{sg} = \frac{m_{sg}}{m_t}, \quad x_f = \frac{m_f}{m_t}$$

The stoichiometric air/fuel ratio is defined as the minimum amount of air required divided by the amount of fuel, and can be calculated for the specific gas:

Equation 3-12

$$\sigma = \frac{m_{a,min}}{m_f}$$

The air excess ratio is defined as the mass of air divided by the minimum amount of air required and is also known:

Equation 3-13

$$\lambda = \frac{m_a}{m_{a,min}}$$

The mass fraction balance can now be written as:

Equation 3-14

$$\frac{m_a}{m_t} = \left(1 - \frac{m_{sg}}{m_t}\right) - \frac{m_f}{m_t}$$

Since $\left(1 - \frac{m_{sg}}{m_t}\right)$ is known, it will be written as B for simplification.

The mass of air and the mass of fuel can be written in terms of the stoichiometric ratio and the air excess ratio in the following way:

Equation 3-15

$$\sigma \cdot \lambda = \frac{m_{a,min}}{m_f} \cdot \frac{m_a}{m_{a,min}} = \frac{m_a}{m_f}$$

Now both sides of the mass fraction equation can be multiplied with the above:

Equation 3-16

$$\frac{m_a}{m_t} \cdot \frac{m_a}{m_f} = B \cdot \frac{m_a}{m_f} - \frac{m_f}{m_t} \cdot \frac{m_a}{m_f}$$

Which, when written in terms of the air mass fraction, stoichiometric ratio, and air excess ratio simplifies to:

Equation 3-17

$$x_a \cdot \sigma \cdot \lambda = B \cdot \sigma \cdot \lambda - x_a$$

When the air mass fraction is singled out, and B is written again as $\left(1 - \frac{m_{sg}}{m_t}\right)$, the final equation for determining the air mass fraction becomes:

Equation 3-18

$$x_a = \frac{(1 - x_{sg}) \cdot \lambda \cdot \sigma}{(\lambda \cdot \sigma) + 1}$$

This air mass fraction is used in the mass balance, as well as in the "properties library" to calculate several properties of the gas in the cylinder.

3-3-2 Fuel specifications

The fuel specifications of the synthesis gas will depend on the mass fractions of the different constituents. The mass fractions of the different species will be the input for the model. With these mass fractions, the total molar weight of the gas can be calculated. One of the main differences with Diesel is the way the lower heating value is calculated. For the gas, the following equation is used:

Equation 3-19

$$LHV = \sum_i \frac{n_i}{n_m} LHV_i$$

In which the subscript 'i' refers to the individual species. This is different from Diesel since the LHV for Diesel is almost completely determined by the C/H ratio.

3-3-3 Heat transfer between gas and wall

The original Diesel model uses Woschni to calculate the heat transfer coefficient. Typically, the three heat transfer modes (conduction, convection and radiation) are all present in the combustion process. The conductive heat transfer is normally simplified by using a constant cylinder wall temperature, which is a good approximation [45]. Also, because of the lack of soot particles in case

of SI engines, the radiation part can be neglected [35], [45]. The only part left is the convective heat transfer part.

The convective heat flux can be described by the following equation:

Equation 3-20

$$\dot{q} = \alpha \cdot \Delta T$$

In which ΔT is the temperature difference between the working fluid and the cylinder wall and α is the convective heat transfer coefficient (W/m^2-K). For the convective heat transfer coefficient, Woschni`s method is used in the original Diesel C model. However, it can be argued that for combustion of synthesis gas this is not the best method to use, but Annand is better.

The convective heat transfer coefficient is derived based on the relationship between the Nusselt (*Nu*), Reynolds (*Re*) and Prandtl (*Pr*) number according to:

Equation 3-21

$$Nu = a \cdot Re^b \cdot Pr^n = a \cdot Re^b$$

In which the superscripts are constants to be chosen.

The above formulation has been adjusted and tuned based on various experimental data for conventional hydrocarbon based fuels. Annand has come with the following formulation for the convective heat transfer coefficient:

Equation 3-22

$$\alpha = a \cdot \frac{k}{D_b} \cdot Re^{0.7}$$

In which

Equation 3-23

$$Re = \frac{p \cdot c_m \cdot D_b}{R \cdot T \cdot \eta}$$

Here c_m is the mean piston speed and η is the dynamic viscosity. *k* is the conductive heat coefficient of the material. It is clear that the transport properties like thermal conductivity and viscosity are very much present in the formulation. This means that when the mixture changes, the transport properties change and thus the heat transfer coefficient will change.

Woschni has given the following formulation for the heat transfer coefficient, as also derived by Stapersma [44]:

Equation 3-24

$$\alpha = 130 \cdot \frac{1}{{D_b}^{0.214}} \cdot \frac{p^{0.786}}{T^{0.525}} \cdot (C_3 \cdot c_m + C_4 \cdot \frac{p - p_0}{p_1} \cdot \frac{V_s}{V_1} \cdot T_1)^{0.786}$$

It can be seen that the transport properties in Woschni`s formulation have been incorporated in the tuneable coefficients. Since this formulation is tuned for conventional fuels which use a high air/fuel ratio, the heat transfer coefficient would not be correct anymore for synthesis gas like producer gas, which have an air/fuel ratio of almost 1. Since this research is looking into the influence of the thermophysical properties of producer gas on the engine performance, the formulation as given by Annand is preferred over Woschni. Annands formulation is therefore incorporated in the Diesel C model.

The difference in heat transfer coefficient between air and producer gas is clear from Figure 16. It shows that the heat transfer coefficient for producer gas is much higher than for air, which means that the heat transfer coefficient for the mixture of PG and air, with an air/fuel ratio of almost 1, will for sure be higher than conventional fuels with a large air/fuel ratio. Therefore also Shivapuji uses Annand`s formulation instead of Woschni`s [43].

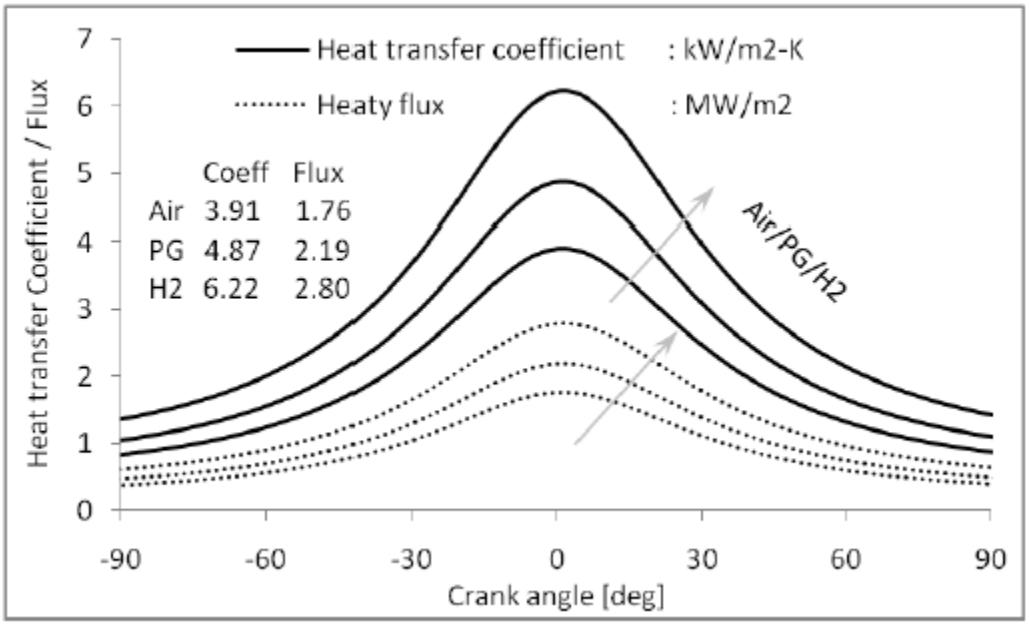

Figure 16: Variation of convective heat transfer coefficient with crank angle for air, PG and H2. After [44]

3-3-4 Thermal conductivity and viscosity

Since Annands formulation is used for the convective heat transfer coefficient, the thermal conductivity and viscosity need to be calculated. When components in a mixture have nearly the same molecular weight, the viscosity of a mixture can be calculated by summing the products of

the viscosities of the individual components and their mole fractions [46]. When this is not the case, mixture viscosities can be quite different. Wilke [47] proposed another formulation, derived by basic kinetic theory, and requires a coefficient φ_{ij} for each pair of components in the mixture:

Equation 3-25

$$\phi_{ij} = \frac{\left[1 + \left(\frac{\mu_i}{\mu_j}\right)^{1/2} \left(\frac{M_j}{M_i}\right)^{1/4}\right]^2}{\left(\frac{4}{\sqrt{2}}\right)\left[1 + \left(\frac{M_i}{M_j}\right)\right]^{1/2}}$$

In which:
$\mu_{i,j}$ = specie viscosity
$M_{i,j}$ = molecular weight

The mixture viscosity can then be calculated using:

Equation 3-26

$$\mu_{mix} = \sum_{i=1}^{i=n} \frac{\mu_i}{\frac{1}{x_i} \sum_{j=1}^{j=n} x_j \phi_{ij}}$$

The mixture thermal conductivity is calculated using:

Equation 3-27

$$\lambda_{mix} = \frac{1}{2}\left[\sum_{i=1}^{i=n} x_i \lambda_i + \frac{1}{\sum_{i=1}^{i=n} \frac{x_i}{\lambda_i}}\right]$$

For the individual species viscosity and thermal conductivity, NASA [48] has made curve fit coefficients available. The general formulation for the specie transport properties is the following:

Equation 3-28

$$\ln(k) = A_k \ln(T) + \frac{B_k}{T} + \frac{C_k}{T^2} + D_k$$

Equation 3-29

$$\ln(\mu) = A_\mu \ln(T) + \frac{B_\mu}{T} + \frac{C_\mu}{T^2} + D_\mu$$

Since the NASA coefficients are also available for the specific heat at constant pressure, these coefficients are also adopted for calculating the individual specie specific heat according to:

Equation 3-30

$$\frac{C_{p_i}}{R_u} = a_1 T + a_2 T + a_3 T^2 + a_4 T^3 + a_5 T^4$$

The mixture specific heat is calculated according to:

Equation 3-31

$$C_{p_{mix}} = \sum_{i=1}^{i=1} x_i C_{p_i}$$

Using the above formulations, the thermophysical properties of the mixtures are very much specie dependent, which should give more accurate results than using conventional methods based on conventional fuels. The properties are calculated based on the molar fractions of the species in an excel file, after which a polynomial function is calculated in Matlab. Annand is then added to the Simulink model instead of Woschni, as can be seen in Figure 17.

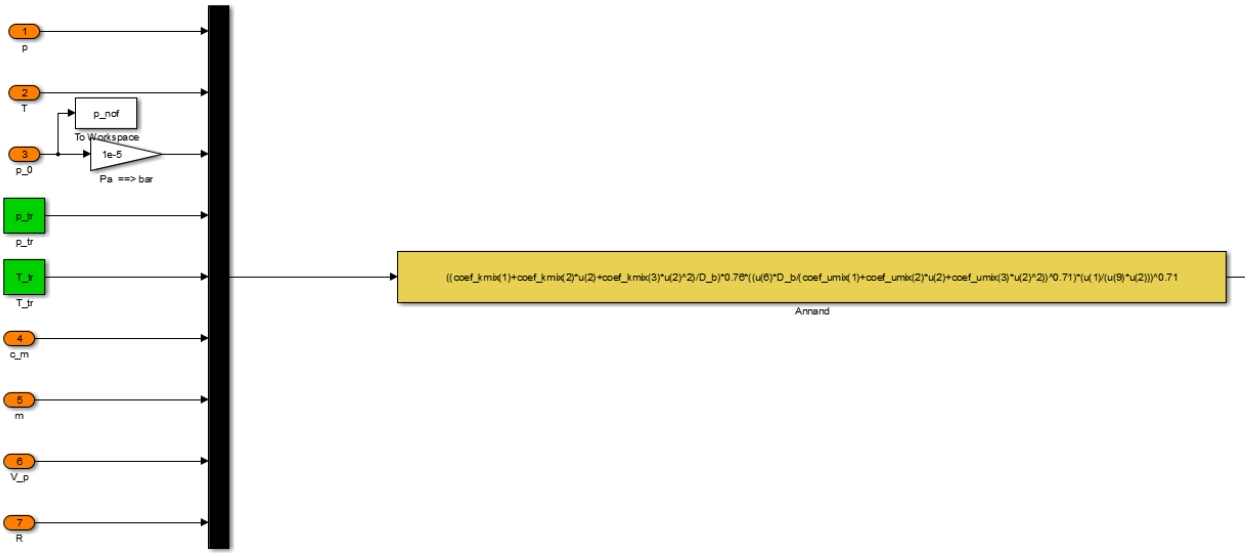

Figure 17: Annand in Simulink

With the model being changed to a SI engine and further changed to simulate syngas type gases, the model can now be verified with data from found literature.

4 Matching the model with literature data

In this Chapter the modified Diesel C model will be matched with different experimental results from different studies. This is done to verify if the model is correct. Once the model is correct, it can then be further used for the simulation of anode-off gas combustion. The first study is conducted by dr. Annand Shivapuji [43]. His study used producer gas as fuel, which is similar to anode-off gas as previously explained. First the data will be given which comes from his experiments. After this, the simulation results with this data as input will be compared to the experimental results. The differences will then be discussed, and it will be assessed if the model is correct. Then the results from a second study, also conducted by Shivapuji but on a different engine, will be compared to the simulation results.

4-1 Experimental data from literature

Most data is available on a turbo charged, after cooled, 6 cylinder engine (E6). It is originally a diesel engine, which has been converted to SI operation. The basic geometric specifications are given in Table 5.

Table 5: Geometric specifications of engine E6 used in experiments

Geometric specifications			**Model input**
	units		
Number of cylinders	-	6	Yes
Bore	*mm*	102.0	Yes
Stroke	*mm*	120.0	Yes
Displaced Volume	*L*	5.9	No
Connecting Rod	*mm*	192.0	Yes
Piston bowl type	-	Cylindrical	No
Bowl depth	*mm*	19.0	No
Bowl top diameter	*mm*	72.0	No
Bowl base diameter	*mm*	72.0	No
SI mode specifications			
Engine speed	*RPM*	1500	Yes
Compression ratio	-	10.5	Yes

The above data has been used as input in the geometric data part in the driver.m file in the Matlab model. Since it is a 4-stroke engine, k=2. Other than the geometric data, the following information was provided on the engine and the experiments:

Table 6: General data on engine E6 experimental conditions

General data on engine E6 experimental conditions			Model Input
	units		
EVC	°	33 after TDC	Yes
EVO	°	115 after TDC	Yes
IVC	°	218 after TDC	Yes
IVO	°	13 before TDC	Yes
P1	*bar*	2.05 +/- 0.1	Yes
T1	*K*	325 +/- 3	Yes
SOC	°	9 +/- 1.5 BTDC	Yes
EOC	°	32 +/- 2 ATDC	Yes
A/F ratio	-	1.3 +/- 0.05	Yes
Air excess ratio	-	1 +/- 0.075	Yes
Stoichiometric gas fraction	-	0.037	Yes
m1	*kg*	0.0020044	Yes
R1	*J/kg-K*	310.23	Yes
BSFC	*Kg/kWeh*	2.5 +/- 0.13	No
Vibe parameter a	-	2.3	Yes
Vibe parameter m	-	0.7	Yes

Besides the above data, also a pressure-crank angle curve, mass burn fraction curve and heat release fraction curve are available from the experiments. These curves have been extracted and loaded into Matlab. The simulation is run with the above parameters, and the mentioned curves are compared to the curves of the experiments. The results can be seen in the next section. These simulation results have been achieved with the above parameters, although some have been changed within the deviations given by Shivapuji:

Table 7: Input parameters simulation

Input parameters simulation		
	units	
P1	*bar*	1.95
T1	*K*	328
SOC	°	7.5 BTDC
EOC	°	33.5 ATDC
A/F ratio	-	1.35
Air excess ratio	-	0.94

4-2 Simulation results engine E6 turbocharged

4-2-1 Pressure trace

All the changes made to the parameters are within the deviations given by Shivapuji. The pressure-crank angle curve from the simulation is a close match with the experimental results. In the compression stroke, the simulated pressure seems to go up faster than the experimental pressure curve. A reason for this could be that the heat loss during the experiment is higher compared to the simulation, resulting in a higher simulated pressure. The experimental and simulated pressure trace can be seen in Figure 18.

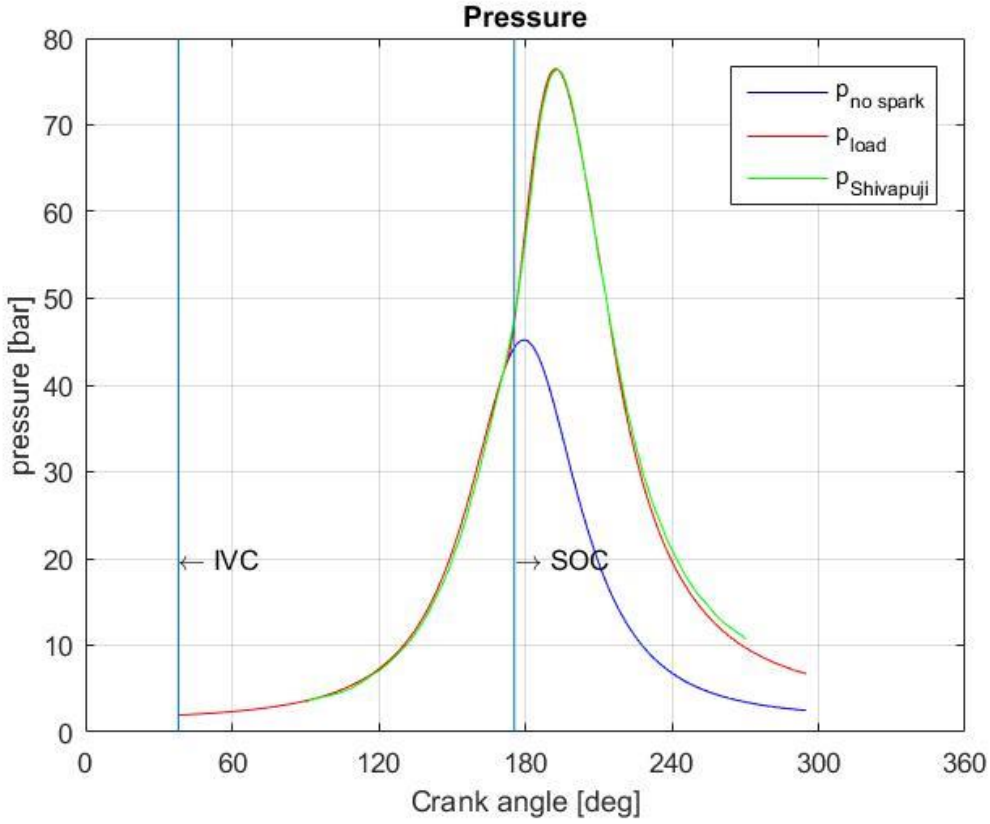

Figure 18: pressure trace simulation and experiment E6 TA:

The simulated peak pressure occurs 1 degree crank angle earlier than the experimental peak pressure. This could be explained by the inaccuracy during the extraction of the experimental pressure curve, since this was done using extraction software which requires you to click on a point on the curve. The simulated peak pressure is 76.26 bar and the experimental peak pressure is 76.23 bar. The peak pressure only deviates less than 0.01% between the two pressure curves.

To get a better idea of the difference between simulation and experimental results, the pressure difference is plotted in Figure 19. The biggest difference in bar occurs right after TDC, where the difference is almost 2 bar. This is logical since the pressure rise rate at this point is the highest, which means that a small difference between the 2 graphs will cause a relatively large difference in absolute pressure. The underprediction in the expansion stroke can be explained with the normalized fuel burnt, which is shown in Figure 20.

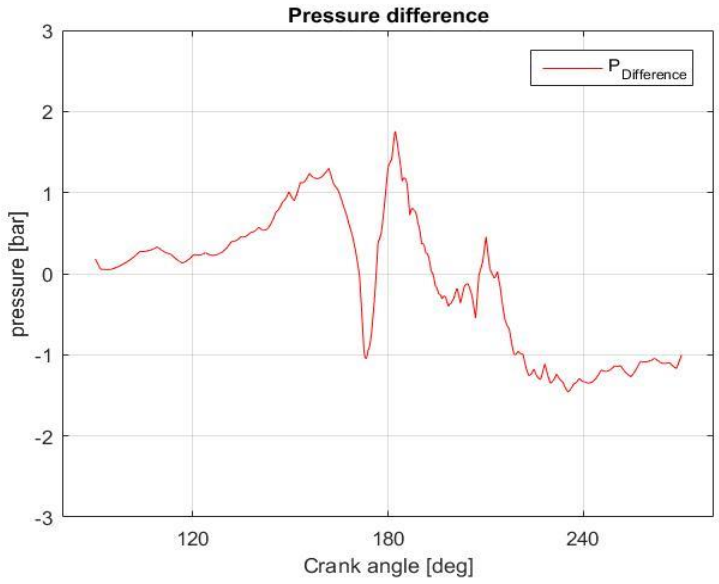

Figure 19: Pressure difference between simulation and experimental results

4-2-2 Normalised fuel burnt

Since the fuel efficiency parameter "a" was given as 2.3, the fuel efficiency comes to 90% as can be seen below. However, the data shows that in the experiment there is still fuel burned, up to 98% efficiency. This would mean that if more fuel is still burned, the pressure will stay higher. Another thing to note is that the fuel burning rate seems to be slightly faster for the experimental data than for the simulation, and the start of combustion seems to be closer to 9 degrees BTDC. However, with this is input, the simulation seems to go further away from the experimental data, and therefore it is chosen to work within the allowed deviations as given to get the model as close as possible.

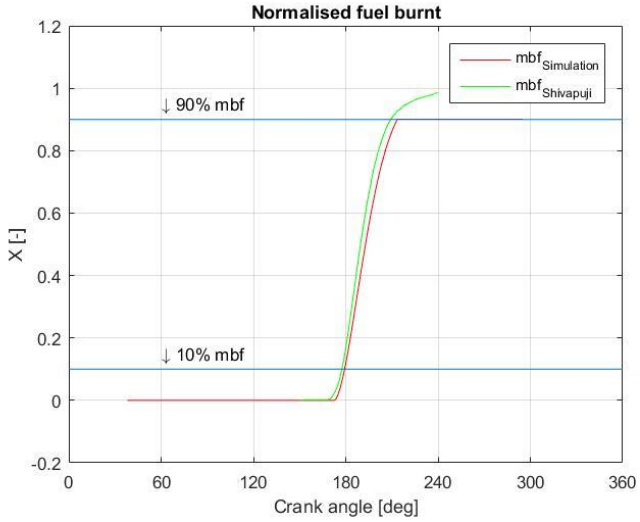

Figure 20: normalized fuel burnt

4-2-3 Convective heat transfer coefficient

The convective heat transfer coefficient can be seen in Figure 21. It is showing both the condition where no fuel is burned and when the mixture is combusted. As can be expected, the heat transfer coefficient is higher when there is combustion. Also, the peak shifts to the right, since the peak temperature is positioned after the TDC as can be seen in Figure 22. What stands out is that the peak of the heat transfer coefficient is more than 20 degrees of crank angle earlier than the peak of the temperature. This makes sense when looking at equation 3-22 and 3-23 which show how the heat transfer coefficient is calculated. All parameters change over time, but the parameter which changes the most is pressure. Therefore the heat transfer coefficient is mainly driven by pressure, and thus follows a similar trend as the pressure and not for example the temperature. The fact that the peak temperature follows after the peak pressure can be explained with a derivation from the basic energy equations. This is not done here since it is not a main point of interest, but it can be found in the study by Stapersma [44].

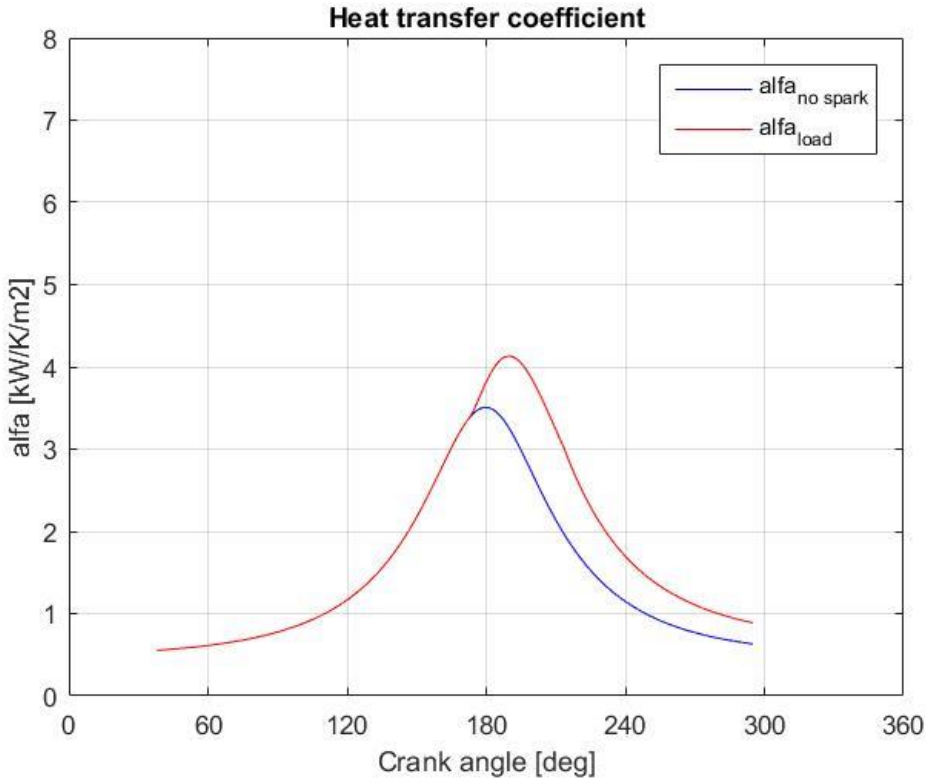

Figure 21: Heat transfer coefficient simulation PG

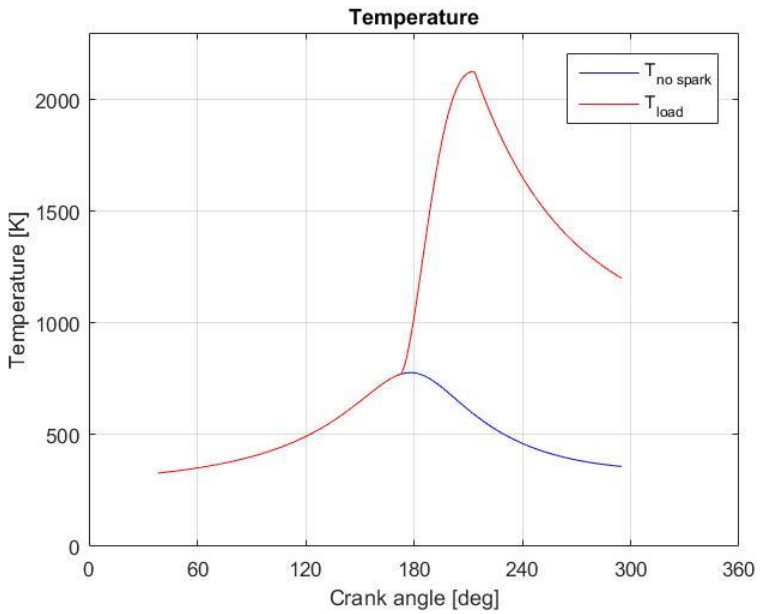

Figure 22:Temperature simulation PG

The change in the mass balance compared to the Diesel mode operation becomes clear with Figure 23. The m_{cyl} is the total mass in the cylinder. As can be seen, the total mass does not change, since the air and gas come into the cylinder in the mixed condition. In a Diesel engine, the fuel would be added later, which would then change the mass in the cylinder after the inlet valve closed. Also note that the $m_{a\text{-}cyl}$, the mass of air in the cylinder, is close to half of the total mass in the cylinder. From the moment of combustion, the mass of air starts to become less, and the stoichiometric gas in the cylinder starts to increase. This trend shows that the new mass balance is working.

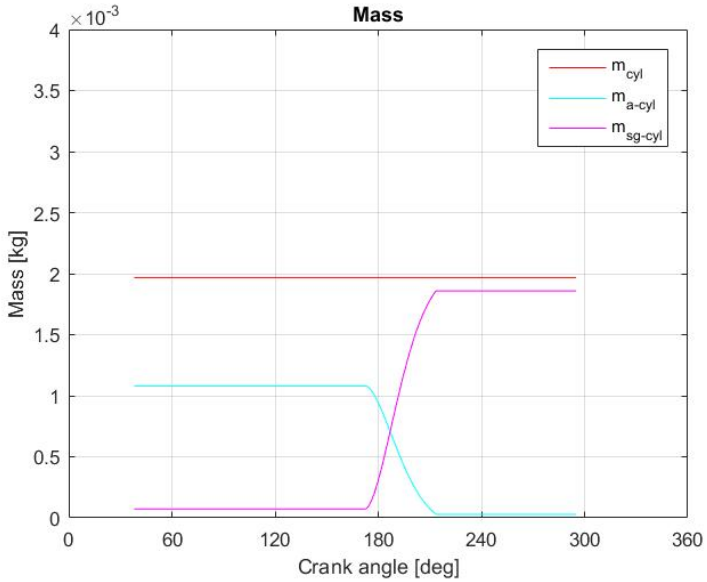

Figure 23: Mass balance simulation PG

4-2-4 Heat release fraction

The model uses the fuel specific Wiebe coefficients as matched by Shivapuji [44]. The experimental heat release fraction and the simulated heat release fraction are shown in Figure 24. It shows there is a very good match between the experimental and simulated results.

4-2-5 Specific fuel consumption

Another check to see if the model is working properly, is to compare the specific fuel consumption of the simulation to the experiments. The fuel consumption from the simulation is given in kg/h. It needs to be noted that this is for one cylinder only. The fuel consumption of the experiments is given in kg/kWeh, which means the total fuel consumption from the simulation needs to be divided by the total power, taking into account the conversion efficiencies.

The specific fuel consumption from the simulation is 2.48 kg/kWeh, which falls within the given value of 2.5 kg/kWeh +/- 0.13.

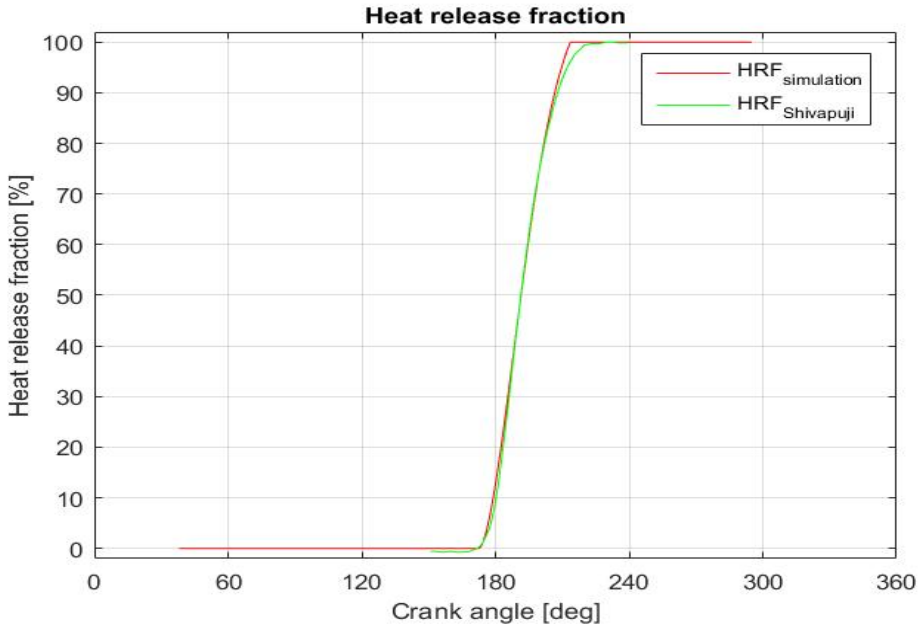

Figure 24: Experimental and simulated heat release fraction

4-2-6 Efficiency

The gas to electricity conversion efficiency for the experiments is given as 29 +/- 1.4 %. The simulated indicated efficiency is 29.8%. This efficiency however does not take into mechanical losses and conversion efficiencies. If a total conversion efficiency of 93% is assumed (95% mechanical, 98% conversion), the total simulated efficiency would be around 27.8%, which falls in the given range.

An overview of the different parameters to compare the experimental results with the simulation results is given in Table 8.

Table 8: Experimental and simulation values E6 TC

Experimental and simulation values			
	units	*Experiment*	*Simulation*
m1	*kg*	0.0020	0.0020
P1	*bar*	2.05 +/- 0.1	1.95
T1	*K*	325 +/- 3	325
R1	*J/kg-K*	310.23	304.6
BSFC	*kg/kWh*	2.5 +/- 0.13	2.48
Peak pressure	*bar*	76.23	76.26
Peak pressure crank angle	°	13.2 ATDC	12.5 ATDC
$\eta_{gas \rightarrow electricity}$	*%*	29 +/- 1.4	28.3
A/F ratio	-	1.3 +/- 0.05	1.35
Air excess ratio	-	1 +/- 0.075	0.94
Peak Temperature	*K*	Not measured	2111
Peak Load	*kWe*	73.8	74.5

4-3 Simulation results engine E4 naturally aspirated

To further verify the model, experimental results from another engine are compared to simulation results. This engine has also been use by Shivapuji in [43]. The engine is a naturally aspirated, 4 cylinder engine adapted for generator application. The CR is 11.2, compared to the 10.5 from the E6 engine. Again, the same type of producer gas is used in this engine. The main data from the engine and input for the model are shown in Table 9. The valve timings are the same as engine E6. The simulated and experimental pressure trace are shown in Figure 25. The pressure difference between the experimental and simulation values are shown in Figure 26.

Table 9: Experimental values engine E4

General data on engine E6 experimental conditions			Model Input
	units		
P1	*bar*	0.919 +/- 0.1	Yes
T1	*K*	312 +/- 3	Yes
SOC	°	5 +/- 1.5 BTDC	Yes
EOC	°	39 +/- 2 ATDC	Yes
A/F ratio	-	1.35 +/- 0.05	Yes
Air excess ratio	-	1 +/- 0.075	Yes
Stoichiometric gas fraction	-	0.037	Yes
R1	*J/kg-K*	310.23	Yes
Vibe parameter a	-	2.46	Yes
Vibe parameter m	-	0.72	Yes

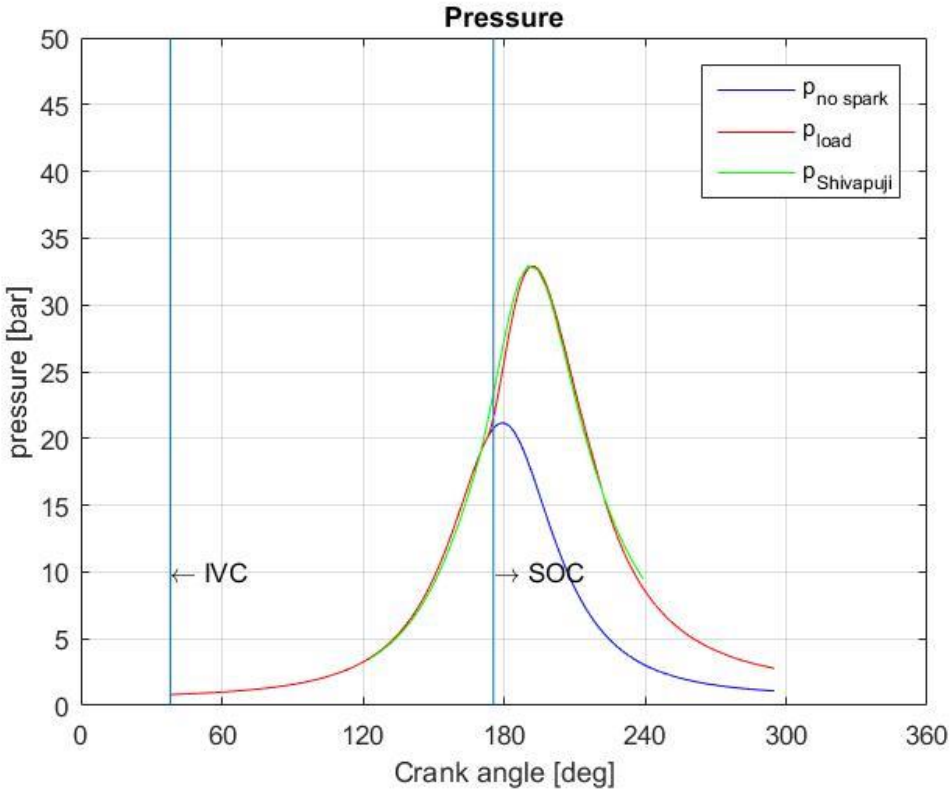

Figure 25:Experimental and simulation pressure trace E4 NA

The simulated pressure trace stays within 1 bar of the experimental pressure trace, except for the region where combustion starts. It seems that the experimental combustion starts earlier than the values given, and here the pressure difference shortly increases to almost 2 bar. To stay within the deviations given, the start of combustion crank angle has not been changed to an earlier crank angle. The experimental and simulation values for engine E4 under naturally aspirated condition are shown in Table 10.

Table 10: Experimental and simulation values for engine E4, NA

Experimental and simulation values			
	units	*Experiment*	*Simulation*
P1	*bar*	0.919 +/- 0.1	0.82
T1	*K*	312 +/- 3	310
Peak pressure	*bar*	32.9	32.9
Peak pressure crank angle	°	11.5 ATDC	12.5 ATDC
$\eta_{gas \rightarrow electricity}$	*%*	Not given	26.7
A/F ratio	-	1.35 +/- 0.05	1.4
Air excess ratio	-	1 +/- 0.075	1
Peak Temperature	*K*	Not measured	2070
BSFC	*kg/kWh*	Not given	2.59
Peak Load	*kWe*	14.5	15.4

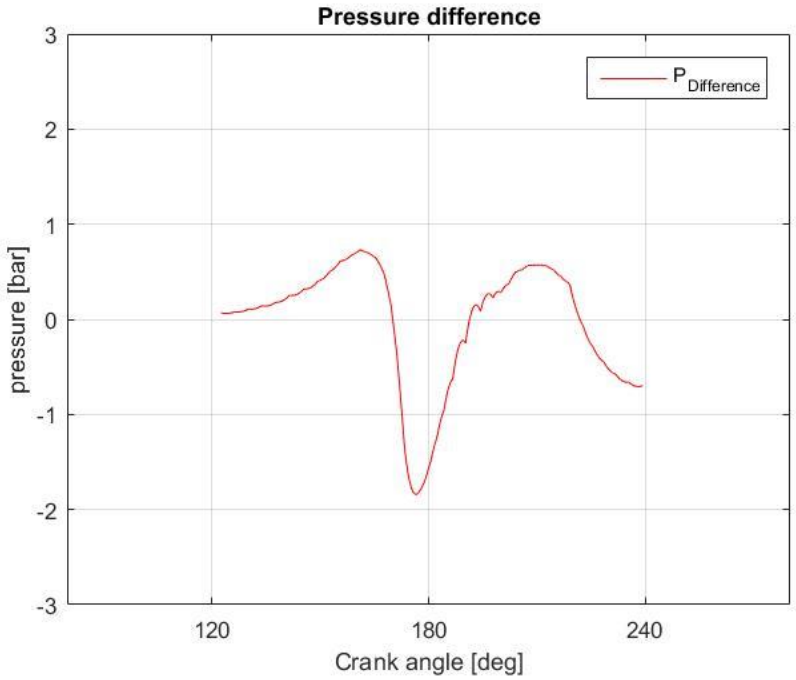

Figure 26: Experimental and simulation pressure difference E4 NA

The difference in the start of combustion becomes more clear when looking at the mass burn fraction in Figure 27. It clearly shows that the fuel starts burning earlier in the experiments, confirming the start of combustion is further before top dead centre than currently is the case.

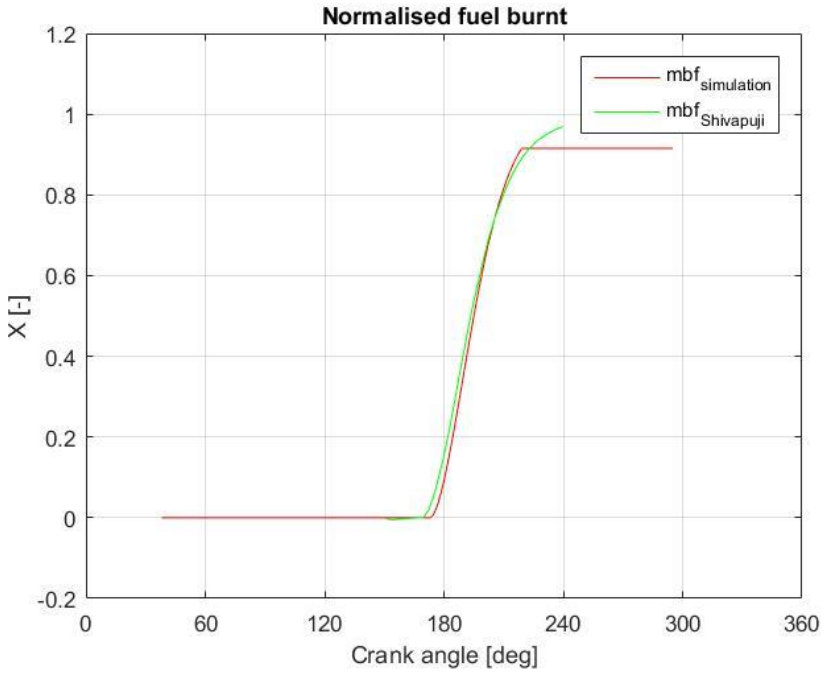

Figure 27: Experimental and simulation mass burn fraction engine E4, NA

4-4 Summary

In this chapter, the developed model has been used to simulate experiments on different engines, conducted by dr. Anand Shivapuji. Only from the engines E6 (turbocharged and naturally aspirating) and E4 (naturally aspirating) enough data was available to verify the model. The model was able to predict the pressure trace for both engines within an acceptable accuracy of 6%. For both the engines E6 TA and E4, the estimated peak load is only 2% and 8% off. There is always an overestimation of the peak load, which can be caused by conversion losses which have not been taken into account. A 95% conversion efficiency from mechanical→electrical has been used, which seems to be too low for these engines. Based on the above results, the model is found to work sufficient and further investigation into anode-off gas will be done with the current model.

5 Determining combustion duration for anode-off gas

In chapter 3 and 4 the engine model has been discussed and verified for syngas, a similar gas as anode-off gas. The idea is to use this adjusted engine model for the simulation of anode-off gas. By using the same engine (E6) as been used by Shivapuji, the output can be compared, and more can be said about the combustion of anode-off gas. However, as discussed in chapter 3, there are still differences between the gases. One of the main differences, which is needed as input for the engine model, is the combustion duration. The change in composition will influence the speed at which the flame will propagate through the cylinder, and thus how fast the fuel will be burned. It is therefore necessary to know what the flame speed of the gas will be.

In this chapter, first more information will be given on the different parts of the combustion to understand better what is happening in the cylinder. After this more details on the influence of H_2 on combustion will be given, since one of the main differences between syngas and anode-off gas is the percentage of H_2. It will be shown that one of the main changes will be found in the speed at which the flame will propagate through the cylinder. Because this seems as a main parameter for the combustion duration, more research is done into the flame speed, and both laminar and turbulent flame speed will be discussed. Both the laminar and turbulent flame speed will be determined for anode-off gas. The link between these flame speeds and the combustion duration will be further elaborated, after which the combustion duration for anode-off gas will be estimated based on flame speed. To come to this combustion duration, several assumptions have been done, which will become more clear throughout this chapter.

5-1 Combustion phases

To understand better what happens inside the cylinder, first the different phases of combustion will be discussed. Typically three combustion phases can be distinguished: The initial development phase (±10% of mass burn fraction), the fast burn phase (±10%-90% of mass burn fraction) and the terminal phase (±90%-98% of mass burn fraction) [45].

5-1-1 Initial development phase

In this phase, a spark is introduced and the flame will start to develop. This development period is called the ignition delay. It is normally taken as the time until 1% of mass is burned [48]. After the initial flame kernel development, the kernel will grow with the laminar flame velocity, until a certain point where it becomes turbulent.

The flame kernel development time depends on the minimum ignition energy required for the fuel (E_{min}). The spark will always provide the same amount of energy, but different fuel types will have different ignition energies. A lower required ignition energy will cause an excess of energy available, which will lead to a larger flame kernel with a higher temperature, transitioning faster into a turbulent flame [49]. For anode-off gas, with a higher H_2 content than producer gas, it can thus be expected that the initial development phase will be shorter than producer gas. The reduction in minimum ignition energy is related to higher mixture reactivity and hence flame speed, which has been shown by [50]:

Equation 5-1

$$E_{min} \propto \rho C_p T \left(\frac{\alpha}{S_L}\right)^3$$

In which:
S_L = the laminar flame speed
α = Thermal diffusivity
ρ = Density
T = Temperature

5-1-2 Fast burn phase

In the fast burn phase, different turbulent combustion regimes can occur. The type of combustion regime depends on the relative size of the turbulent length scales to the laminar flame thickness [51]. When the laminar flame thickness is smaller than the smallest of the turbulence length scales, the influence of turbulence is only to wrinkle the flame surface. On the other hand, when the laminar flame thickness is larger than the largest turbulence length scale, the flame will get stretched so much that pockets will break off, also known as the distributed reaction regime. A mixture between these regimes is also possible. The combustion regime in combustion engines is typically in the wrinkled laminar flame regime, where the mixture consumption rate is driven by the turbulent flame speed. Because of the turbulence, the consumption of fuel is the highest, which explains why this is called the fast burn phase. More on the laminar and turbulent flame speeds will follow later in this chapter.

5-1-3 Terminal phase

In the terminal phase there is a reduction of the rate of heat release, until complete termination of the heat release. After the terminal phase no more fuel is burned and the combustion is over. The influence of fuel composition on the terminal phase will become more clear in the next section.

5-2 Influence of H_2 on combustion phases

Because one the main differences between anode-off gas and syngas is the hydrogen content, more information on the influence of hydrogen on the combustion will be given. A study on the influence of the hydrogen fraction has been done by [44]. Here it was shown that for increasing the amount of hydrogen, both the initial development phase and the fast burn phase are shortened, but the terminal phase takes longer. An overview of the results for different fractions of hydrogen is shown in Figure 28, where SG stands for syngas. SG1 contains 7.1% of hydrogen (in stoichiometric

mixture with air), SG4 contains 14.2% of hydrogen. The initial development phase and fast burn phase are both shortened for higher amounts of hydrogen because of an increase in the laminar flame speed due to the extra hydrogen. However, a higher flame speed also causes enhanced convective losses. At the same time, the flame will reach the much cooler cylinder wall sooner. These factors contribute to a greater part of the fuel to run cooler after the moment of peak pressure, contributing to an increase in the terminal phase combustion duration [43].

Based on the above observations it can be concluded that a similar trend can occur when combusting anode-off gas, since the hydrogen content is higher than for producer gas. A big factor seems to be the flame speed. Therefore the different flame speeds, laminar and turbulent, will now be further discussed to better understand how the combustion duration of anode-off gas can be determined.

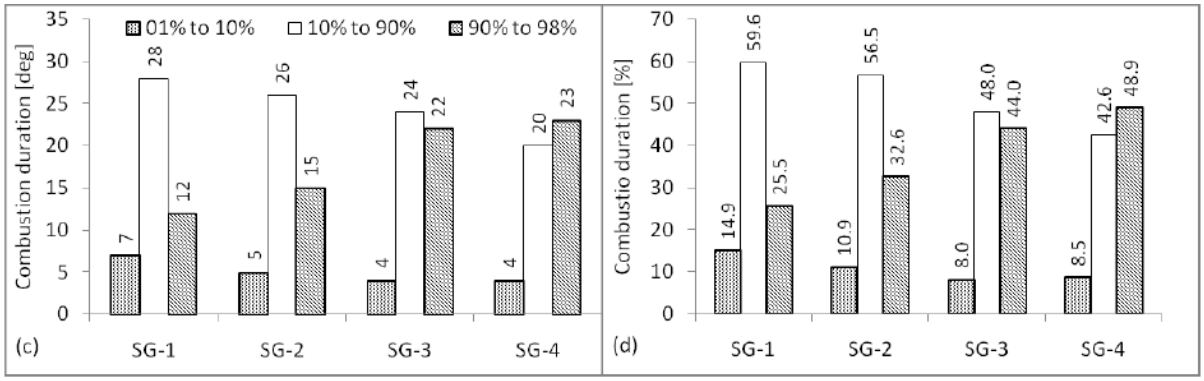

Figure 28: Influence of syngas hydrogen fraction on combustion duration, after [44]

5-3 Laminar premixed flames

The laminar flame speed is defined as the velocity of the unburned gases through the flame front in the direction normal to the flame surface [52]. From the previous sections it is clear that the laminar flame speed has a large contribution on the combustion phases. Ideally there would be a clear relation between the laminar flame speed and the reaction rate, which would say something about how fast the reactions takes place. As will be shown later in this chapter, this is not so straight forward. First a closer look will be given on what happens in the flame. After that, a derivation for the flame speed and the reaction rate will be given. Information in this section has been retrieved through lectures of Prof. S.R. Chakravarthy from IIT, Madras [52]. Figure 29 shows a 2-zone laminar premixed flame, developed by Mallard and Le Chatelier. According to them, the laminar flame propagation is described by the laminar flame speed. The first zone is the preheat region (also convective/diffusive zone) and the second zone is the burning zone (reactive/diffusive zone). The burning zone has a thickness δ, the laminar flame thickness.

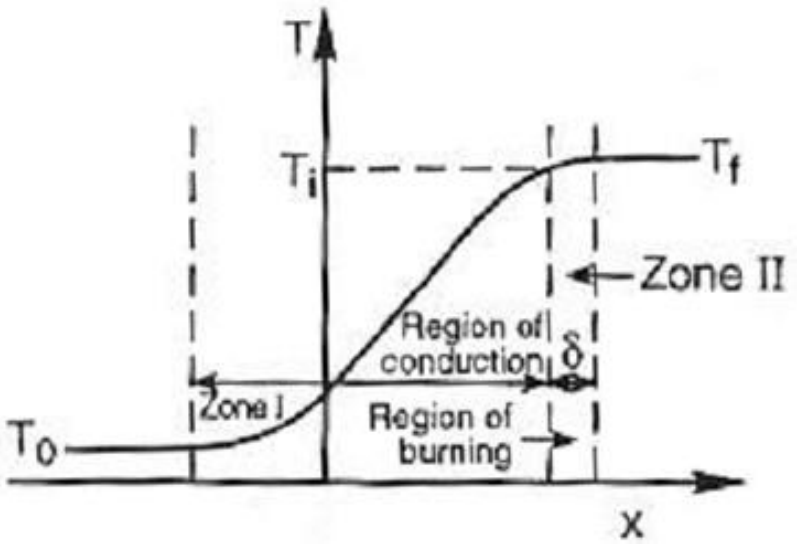

Figure 29: Flame zone regions, after [54]

The flame is moving by the conduction of heat from the burning zone to the preheat zone. The heat conducted raises the temperature of the unburned mixture to the flame temperature. The following equations apply:

Equation 5-2

$$\rho_0 S_L C_p \left(T_f - T_0\right) \approx k \frac{\left(T_f - T_0\right)}{\delta} = \omega Q \delta$$

In which:
k = thermal conductivity
ω = mass of reactants/unit volume/unit time (reaction rate)
Q = heat value of the reaction
T_f = flame temperature
T_0 = unburned gas temperature

This formulation states that the change in enthalpy (left side of equation) is equal to the heat conduction (middle part of equation), which has to balance the heat released due to the chemical reactions (right side of the equation).

Now the global energy balance is:

Equation 5-3

$$C_p \left(T_f - T_0\right) = Q$$

Combining the above equations gives a formulation for the laminar flame speed as a function of the reaction rate:

Equation 5-4

$$S_L = \frac{1}{\rho_0}\sqrt{\frac{\omega k}{C_p}}$$

This shows that the laminar flame speed is directly proportional to the square root of the reaction rate.

5.4 Turbulent premixed flames

Besides laminar flames, also turbulent flames are found in the cylinder. These will be discussed further in this section. The air-fuel enters the cylinder under a higher than ambient pressure, inducing a turbulent flow. This, in combination with the piston moving up and down and therefor causing swirl, creates complicated turbulence in the cylinder. This turbulence interacts with the laminar flame, modifying the flame front and changing the laminar flame into a turbulent one. When the turbulence causes the flame surface to wrinkle, rapid fluctuations will occur on this flame front. The propagation of this mean turbulent flame front is described by the turbulent flame speed S_T [53]. The first person to define the turbulent flame speed was Damköhler who used a mass continuity approach [56]. In Figure 30 an illustration of his approach is given. The mass continuity in this approach is the following:

Equation 5-5

$$\dot{m} = \rho_0 A_0 u_0 = \rho A_T S_L = \bar{\rho} A S_T$$

When the density is assumed constant, the following is true:

Equation 5-6

$$\frac{S_T}{S_L} = \frac{A_T}{A}; \quad \frac{A}{A_0} = \frac{u_0}{S_T}$$

According to Damköhler, the turbulence effect in the small scale turbulent regime is reduced to wrinkling the flame front. This led to a simplified expression for the turbulent flame speed:

Equation 5-7

$$\frac{S_T}{S_L} = 1 + C\left(\frac{u'}{S_L}\right)^n$$

in which u' is the turbulence intensity and n is a constant to be chosen. Since the combustion of producer gas is mainly in the small scale turbulent combustion region, and is assumed that this will be the same for anode-off gas, the above formulation will be used to determine the turbulent flame speed of anode-off gas.

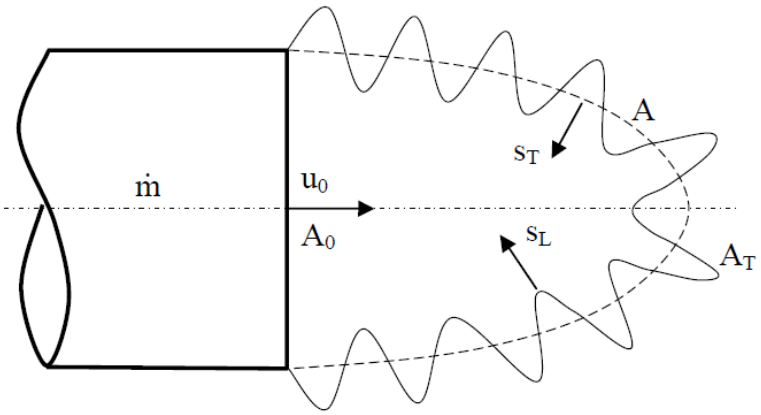

ṁ – inlet mass flow [kg/s]
u_0 – inlet bulk velocity [m/s]
A_0 – inlet surface [m^2]
s_T – turbulent flame speed [m/s]
A – mean flame surface [m^2]
s_L – laminar flame speed [m/s]
A_T – instantaneous flame surface [m^2]

Figure 30: Propagation of the mean and instantaneous turbulent flame front, after [53]

5-5 Laminar flame speed of anode-off gas

Because in the different combustion phases both the laminar flame speed and the turbulent flame speed seem to play a role, both of these will be determined for anode-off gas, after which a link will be tried to make between these flame speeds and the combustion duration. In this section the determination of the laminar flame speed of anode-off gas will be discussed. One way to determine the laminar flame speed is by a 1D approach, which involves detailed chemical kinetics models in which mass, species and energy conservation equations coupled with the chemical reactions are solved. This is an iterative approach where it starts out as a transient problem and is solved until the steady state is reached. This approach is very time consuming and computationally extensive, and therefore out of the scope of this research. Mostly used are the curve fit correlations based on experimental data. This data is based on spherical combustion bomb experiments for various fuels [49], [53] and is generally a function of dimensionless pressure and temperature, as shown below.

Equation 5-8

$$S_L = S_{L_0} \left(\frac{T_u}{T_0}\right)^{\alpha} \left(\frac{P_u}{P_0}\right)^{\beta}$$

This correlation has been further generalized by Keck to incorporate variations in air/fuel ratios [49]. A correlation like this is easy to use, but has certain drawbacks. It is based on experimental data, which means a correlation is not available for every type of fuel and every pressure and temperature. This means that for anode-off gas, such a correlation does not exist.

However, a study with quite similar compositions as anode-off gas has been done by [54]. They have studied the influence of CO_2, CH_4 and initial temperature on the laminar flame speed of a H_2/CO mixture. They varied the volume fractions of H_2/CO (1:3, 1:1, and 3:1 by volume), the CO2 dilution (0%-40%) and the methane fraction (0%-40%). It was found that laminar flame speed increases with increasing H2/CO ratio, while CO2 dilution or CH4 addition decreased it. A correlation for the laminar flame speed was developed based on the experimental data. When

looking at the composition of anode-off gas, it turns out that the laminar flame speed for most of the compositions at different utilization rates can be determined with this correlation. The correlation is the following:

Equation 5-9

$$S_u = S_{L,ref}(1 - c\chi_{CO_2})\left(\frac{T}{300}\right)^a$$

Where:

Equation 5-10

$$S_{L,ref} = S_{L,max} - B(\varphi - \varphi_M)^2$$

In which:

- φ_M = the equivalence ratio at which S_L reaches its maximum
- B = rate of decrease of S_L from its maximum

$S_{L,max}$, B, and φ_M are functions of the volumetric concentration (χ) of CH_4 and of the normalized H2/CO ratio of the syngas defined as:

Equation 5-11

$$R = \frac{\chi_{H_2}}{(\chi_{H_2} + \chi_{CO})}$$

The different parameters are determined with the following formulas:

Equation 5-12

$$S_{L,max} = 2.1\exp\left(-5.9\chi_{CH_4}\right)(R - 0.5) + 1.4\exp\left(-3.97\chi_{CH_4}\right) + 0.4$$

Equation 5-13

$$\varphi_M = -0.905\exp\left(-13.4\chi_{CH_4}\right)(R - 0.5) + 1.05\exp\left(-7\chi_{CH_4}\right) + 1.07$$

Equation 5-14

$$B = \left[-10.5\left(\chi_{CH_4} - 0.2\right)^2 + 1.5\right]R + 3.1\chi_{CH_4} + 0.035$$

Equation 5-15

$$a = \left(1.28 + 0.24\chi_{CH_4}\right) + 0.54(\varphi - \left(1.85 - 3.45\chi_{CH_4}\right))^2$$

Equation 5-16

$$c = 0.028\,exp\left[\left(2.5{\chi^2}_{CH_4} + 1\right)\varphi + 0.5\right] + 1.23$$

With the above formulations, the flame speed of anode-off gas for different utilization rates can be calculated for composition 1. The laminar flame speeds at 300 K can be found in Table 11. Care should be taken with the laminar flame speed for the 85% fuel utilization rate, since the composition falls just outside of the range of the laminar flame speed correlation.

Table 11: Laminar flame speeds at 300 K for anode-off gas

Laminar flame speeds at 300 K for anode-off gas composition 1 at stoichiometry (m/s)				
Fuel utilization rate	85%	75%	60%	50%
Laminar flame speed	0.34	0.68	1.02	1.91

5-6 Turbulent flame speed for anode-off gas

As seen before in this chapter, the turbulent flame speed depends on the laminar flame speed as well as the turbulent intensity and some constants according to the formula by Damköhler. To be able to say something about the combustion duration for anode off gas, especially during the fast burn phase, the turbulent flame speed needs to be known. Therefore the turbulence intensity needs to be known. In the study conducted by Shivapuji the ratio of S_T/S_L is given as a function of the turbulence intensity over the laminar flame speed for the turbocharged E6 engine [44]. From the experimental data it becomes clear that both constants are equal to one, and the formula is reduced to:

Equation 5-17

$$\frac{S_T}{S_L} = 1 + \frac{u'}{S_L}$$

which further simplifies to:

Equation 5-18

$$S_T = S_L + u'$$

For the E6 turbocharged engine S_T/S_L is given. It varies slightly with crank angle between 8.5 and 9.5. For the ease of using a simple relation in the simulation, the ratio is averaged over crank angle and is taken as 9. The laminar flame speed at ambient conditions for producer gas is also known (0.5 m/s) thus the turbulence intensity can be calculated, which in this case is 4 m/s. For the simulation of anode-off gas, the same engine will be used. Therefor it is assumed that the turbulence intensity will stay constant, and can be used for the simulation of anode off gas. A few remarks need to be taken into account with adopting this method:

5-6-1 Turbulence intensity

The value for the turbulence intensity is assumed to stay constant. In reality this will not be entirely true, since it depends on many factors. However, with the engine speed staying the same, and the inlet pressure and valve timing staying the same, the in-cylinder turbulence due to geometry will

stay the same. Also, the influence of the difference in gas composition on the turbulence intensity, is only minor when the combustion takes place close to stoichiometry [51]. Since the engine will be running at the same speed, and anode-off gas will combust at close to stoichiometric conditions, it is a valid assumption to see the turbulent intensity as a constant.

5-6-2 Laminar flame speed at ambient condition

Another remark needs to be made about which laminar flame speed to use. First of all, the aim is to find to combustion duration of anode-off gas, relative to the combustion duration of producer gas. This way the results can be compared to a set of known results. The laminar flame speed can depend on both temperature and pressure. With a higher temperature than ambient conditions, which will for sure occur at the start of combustion, the laminar flame speed will be higher as well. The important thing is to take the laminar flame speed for anode-off gas and producer gas both at the same temperature and pressure. This way, the change in ratio of $S_{T,PG}/S_{T,AOG}$ will stay the same. Secondly a point can be made that different compositions will act differently when the temperature or pressure is changed. In other words, one gas might go up 50% in laminar flame speed where another gas might go up 100% in laminar flame speed, with the same increase in temperature. The main difference between anode-off gas and producer gas is the higher H_2 content in anode-off gas, and CO_2 instead of N_2. Since both N_2 and CO_2 are considered inert gasses, the influence of interchanging these two gasses is assumed to be negligible. The higher H_2 content could however make a difference.

In Table 12 the laminar flame speeds of the four different syngasses as discussed in Chapter 6-2 are shown for ambient conditions (300 K and 1 bar) and engine like conditions (700K and 25 bar). Also the ratio`s between the laminar flame speeds have been calculated and are shown in Table 13. It can be seen that the ratios are hardly different between ambient and engine like conditions. The correlation formula for the laminar flame speed used for anode-off gas is not valid for higher temperatures and pressures. It is therefore chosen to use the laminar flame speed at ambient conditions in the calculations.

Table 12: Laminar flame speeds at ambient and engine like conditions, after [44]

	S_L at 300K, 1 bar	**S_L at 700K, 25 bar**
SG1	14.7	27.5
SG2	27.1	49.8
SG3	37.7	65.5
SG4	54.4	94.2

Table 13: Ratios of laminar flame speeds

	300K, 1 bar	**700K, 25 bar**
SG2/SG1	1.84	1.81
SG3/SG2	1.39	1.32
SG4/SG3	1.44	1.44

Now that the turbulent flame speed can be calculated, it can be compared to the turbulent flame speed of producer gas in the same engine. The flame speed is directly related to how fast the gas is consumed, and therefore the combustion duration. With the ratio of turbulent flame speed, the ratio

of combustion duration between anode-off gas and producer gas is now also known, thus the combustion duration for the fast burn phase of anode-off gas is known.

5-7 Laminar vs turbulent combustion phases

The original idea was to assume the initial development phase as a laminar burning phase, after which the fast burn phase could be treated as turbulent combustion. The terminal phase can be disregarded, when the combustion efficiency is assumed to be similar to producer gas (90%). The combustion duration for the fast burn phase will then be related to the change in turbulent flame speed. The combustion duration of the first 10% of mass burned can be related to the change in reaction rate (RR), which can be calculated through the laminar flame speed using the formula from chapter 6-3.

The above idea has been used to check the combustion duration results for the 4 different syngasses. In Table 14 the results are shown, with the first phase calculated through the reaction rate, and the second phase through the turbulent flame speed.

Table 14: Calculated combustion duration for different syngasses

	S_L (m/s)	S_T (m/s)	$S_{T,x}/S_{T,1}$	RR_x/RR_1	CD 0-10% experiment	CD 0-10% calculated	CD 10-90% experiment	CD 10-90% calculated
SG1	0.15	1.03	1.00	1.0	7	7.0	28	28
SG2	0.27	1.15	1.12	3.4	5	1.5	26	25
SG3	0.38	1.26	1.22	4.9	4	0.8	24	23
SG4	0.54	1.43	1.39	10.0	4	0.4	20	20

From Table 14 it is clear that the adopted method for the fast combustion phase gives similar results as the experimental values, with only 1 degree crank angle difference. The adopted method for the first combustion phase does not seem valid. There can be multiple reasons for this. First of all the fact that the reaction rate is 10 times as fast, does not mean that the actual combustion will also happen 10 times as fast. This combustion is limited by how fast the heat can be transferred, and thus by the thermophysical properties of the gas [51]. Another reason is that the assumption that the first phase is fully laminar might not hold. There is no change at 10% mass burn fraction, and reaching turbulent combustion could be much sooner. Also, there is still turbulence in the cylinder due to the piston moving and the air-fuel mixture entering the cylinder.

In Figure 31 the normalized fuel burnt from the experiments is shown. The graph is close to linear between 10-90%, again confirming the assumption that the turbulent flame speed can be used, and can be averaged over this combustion period. The graph continues with the same inclination below the 10% line, until about 3-4%. This shows that turbulent combustion occurs much earlier.

The same method used for calculating the 10-90% burn phase has also been tried for the 0-10% burn phase. Results are shown in Table 15. The results are much closer to the experimental value than the previous adopted method, with only 1 degree crank angle as maximum difference. Therefore, the ratios between the turbulent flame speeds will be used over the entire range from 0-90% for the calculation of the combustion duration of anode-off gas.

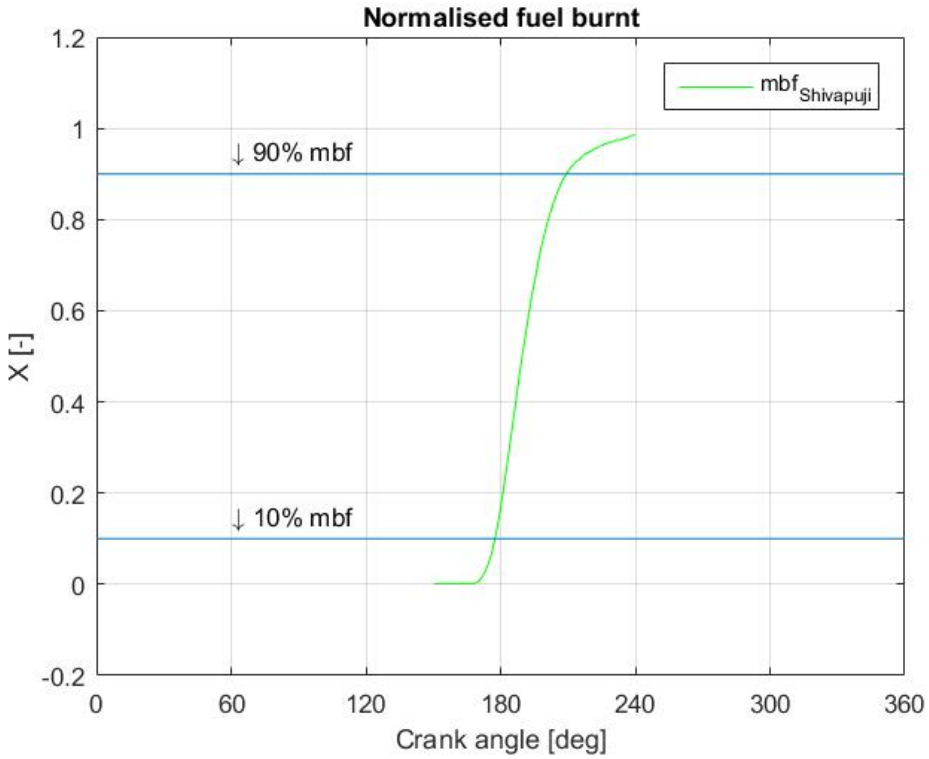

Figure 31: normalized fuel burnt, experimental E6 TA

Table 15: calculated combustion duration 0-10% based on turbulent flame speed ratio

	S_L (m/s)	S_T (m/s)	$S_{T,x}/S_{T,1}$	CD 0-10% experiment	CD 0-10% calculated
SG1	0.15	1.03	1.00	7	7
SG2	0.27	1.15	1.12	5	6
SG3	0.38	1.26	1.22	4	5
SG4	0.54	1.43	1.39	4	5

5-8 Combustion duration anode-off gas

With the adopted method, the combustion duration for different fuel utilization rates of anode-off gas have been calculated. These are shown in Table 16. For comparison reasons, the combustion duration of producer gas is also shown. It shows a clear decrease in combustion duration with increasing flame speed.

Table 16: Calculated combustion duration for anode-off gas

	Combustion duration 0-90% of mass burn fraction, given in crank angle
PG	38
AOG,85	39.4
AOG,75	36.5
AOG,60	34
AOG,50	28.9

5-9 Summary

Typically three combustion phases can be distinguished: The initial development phase (±10% of mass burn fraction), the fast burn phase (±10%-90% of mass burn fraction) and the terminal phase (±90%-98% of mass burn fraction). A study into the effect on the combustion phases of addition of hydrogen has been done by Shivapuji [43]. It was shown that for increasing the amount of hydrogen, both the initial development phase and the fast burn phase are shortened, but the terminal phase takes longer. The original idea was to assume the initial development phase as a laminar burning phase, after which the fast burn phase could be treated as turbulent combustion. The terminal phase can be disregarded, when the combustion efficiency is assumed to be similar to producer gas (90%). Both phases however seem to be turbulent. Therefore the total combustion duration can be linked to the turbulent flame speed, which is a function of laminar flame speed and turbulent intensity. With assuming the turbulent intensity to stay constant, the turbulent flame speed can be calculated and the combustion duration can be calculated using the ratio of turbulent flame speeds between two gasses. The laminar flame speeds of anode-off gas and their combustion duration in engine E6 are given in Table 17.

Table 17: Calculated combustion duration and laminar flame speed for anode-off gas

	Combustion duration 0-90% of mass burn fraction, given in crank angle	Laminar flame speed at stoichiometry (m/s)
PG	41	0.5
AOG,85	42.5	0.34
AOG,75	39.4	0.68
AOG,60	36.7	1.01
AOG,50	31.1	1.91

6 Results

In this chapter, the results of simulating the combustion of anode-off gas will be given. The gas will be used in the E6, turbocharged engine, as used in experiments by [44]. There are four different fuel utilization rates of anode-off gas that will be used. The aim is to compare the anode-off gas to producer gas. In order to compare, several parameters need to stay constant. Once these parameters are set, the model can be run with different fuel utilization rates of anode-off gas. The main properties of the different compositions of anode-off gas and producer gas will be given. The results of the simulations will be compared to producer gas on output such as power, peak pressure, temperature and efficiency. After the results are given, a detailed analysis of these results will be conducted, after which a discussion will follow.

6-1 Choice of constant parameters

Because anode-off gas is simulated in the same engine as producer gas, some parameters have stayed the same. Also, to make a good comparison, some parameters need to stay the same. The following choices have been made:

- Engine geometry, valve timing and speed stays the same
- The combustion will take place under stoichiometric conditions
- The SOC will stay constant
- T_1 = 328 K (same as PG)
- P_1 = 1.95 bar (same as PG)
- Vibe parameters stay the same as PG
- Stoichiometric gas mass fraction from previous cycle (x_{sg}) = 3.7%

Since the AOG will be compared to results from PG, of which the bulk of experimental data is available for one engine, it is only logical to use the same engine with the same speed and valve timing in the simulations. Changing any of this would have many implications, and assumptions that will be made will not hold.

Combustion under stoichiometric condition has been chosen since this is also the case for PG. This has been chosen for producer gas since the mixture lower heating value of PG is already lower than conventional fuels. Increasing the air excess ratio would only lower the mixture LHV more, resulting in power loss from the engine. Another reason to use stoichiometric combustion is that this gives the least possible change of the turbulent intensity due to changes in composition [50]. The same temperature as PG is used to keep the initial conditions close to PG, to have a comparable situation. The same applies for the pressure. The inlet pressure depends on the turbocharger, which depends on the mass flow of a certain composition through the turbine. However, in [43] they were able to match a turbocharger to changing fuel composition to still ensure a high enough inlet

pressure. It is assumed that with the change in composition from PG to AOG this would also be possible.

The Vibe parameters are kept the same as well. The Vibe parameter a is derived from the combustion efficiency and says how much of the fuel in the cylinder is actually burned. For PG in the E6 TA engine, this parameter has been derived through analysis of the exhaust gasses. Using the same engine with the same valve settings, and operating also at stoichiometry, it is assumed that the combustion efficiency of AOG will be similar to that of PG. The Vibe parameter m is the shape parameter, which is normally used to shape the simulated heat release to the experimental heat release. Estimating the heat release profile for different boundary conditions, for example spark timing or pressure, or even a completely different engine are generally not possible [57]. No experimental data is available for AOG. By using the same inlet conditions (temperature and pressure) and the same engine, boundary conditions are set such that using the same value for m as used for PG is justifiable. The start of combustion will first be kept constant. With keeping the start of combustion constant, the influence of the longer/shorter combustion duration for anode-off gas can be made visible.

The stoichiometric gas mass fraction from the previous cycle has been given for PG. With a similar combustion efficiency, engine geometry, valve timing and inlet pressure, there is no reason to assume that this value will change much, and as such be kept constant. With the above parameters set, simulations can be done on AOG. To understand differences in the output more, an overview of the main properties of the different gasses is given in Table 18.

Table 18: Main properties of PG and AOG

Parameter	Units	**PG**	**AOG85**	**AOG75**	**AOG60**	**AOG50**
H_2	*%*	18	30.8	42.2	53.2	58.3
CO	*%*	19	10.8	15.6	21.6	25.1
CO_2	*%*	12	58.4	42.2	25.2	16.6
N_2	*%*	49.2	-	-	-	-
CH_4	*%*	1.8	-	-	-	-
LCV	*MJ/Nm^3*	4.57	4.68	6.53	8.47	9.46
ρ	*Kg/m^3*	1.023	1.306	1.048	0.788	0.663
σ	-	1.3	0.88	1.53	2.67	3.56
S_L	*m/s*	0.5	0.34	0.68	1.02	1.91

6-2 Results of simulation

In this chapter the results of the simulations of the different fuel utilization rates of anode-off gas are given. First several graphs are given, showing the pressure traces, heat release fractions, temperatures and more. After that, these result are analysed.

6-2-1 Pressure traces

In Figure 32 the pressure traces for the different anode-off gasses are given as well as the pressure trace for producer gas in engine E6.

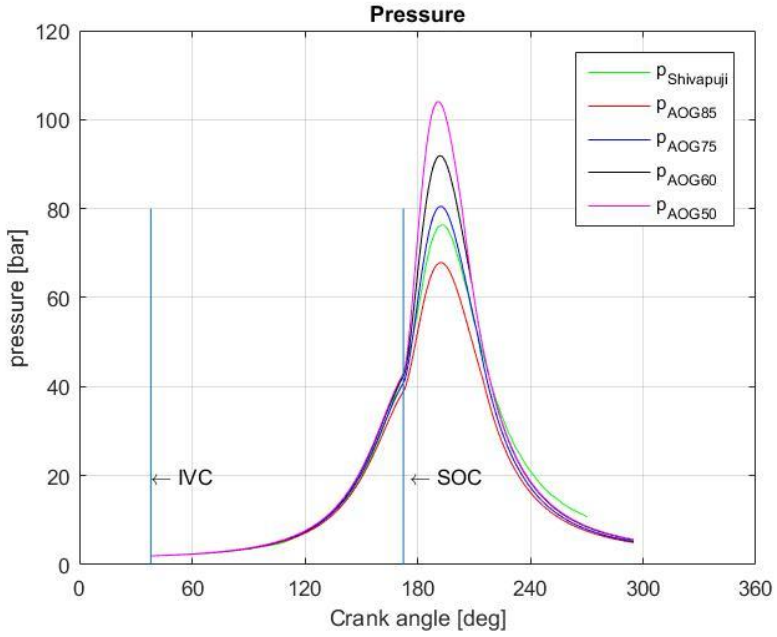

Figure 32: pressure traces anode-off gas

As can be seen, lower fuel utilization rates of anode-off gas have a higher peak pressure. The peak pressure for AOG85 is 68 bar, which increases to 104 bar for AOG50. What also shows it that the position of peak pressure is slowly shifting to the left for lower fuel utilization rates.

6-2-2 Temperature

In Figure 33 the temperature for the different anode-off gasses is shown. The peak temperature increases with lower fuel utilization rates of anode-off gas. Also the peak temperature shifts further to the left for lower fuel utilization rates of anode-off gas. The peak temperature for AOG85 is 2652K, and for AOG50 it is 2847K. The peak temperature of producer gas, when simulated in the same engine model, was 2111K.

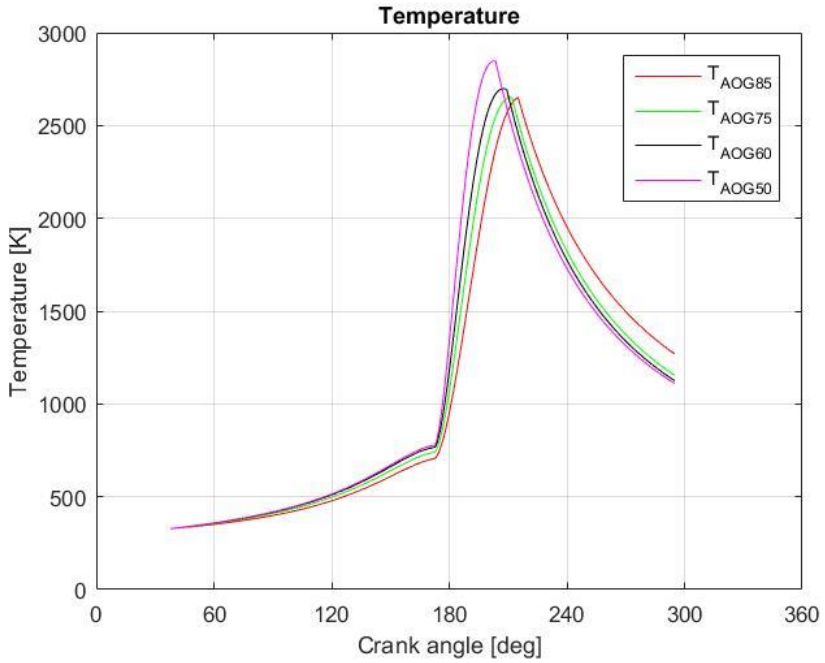

Figure 33: Temperature different anode-off gasses

6-2-3 Heat release fraction

Figure 34 shows the different heat release fractions of anode-off gas. As the fuel utilization rate becomes lower, the heat release fraction curve goes up faster.

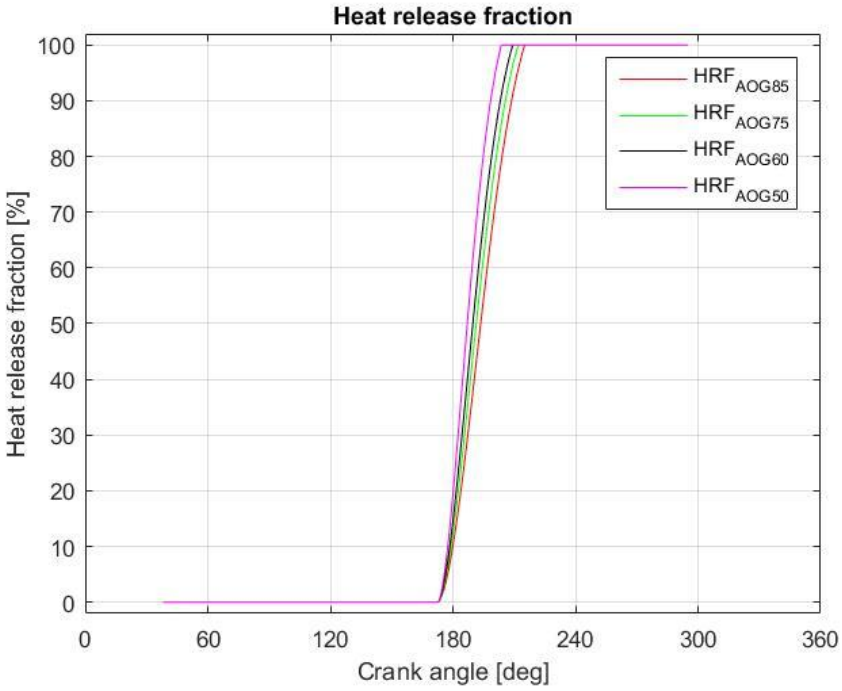

Figure 34: Heat release fractions different anode-off gasses

6-2-4 Heat transfer coefficient

In Figure 35 the heat transfer coefficients are shown for the different fuel utilization rates of anode-off gas. With lower fuel utilization rates, the heat transfer coefficient increases.

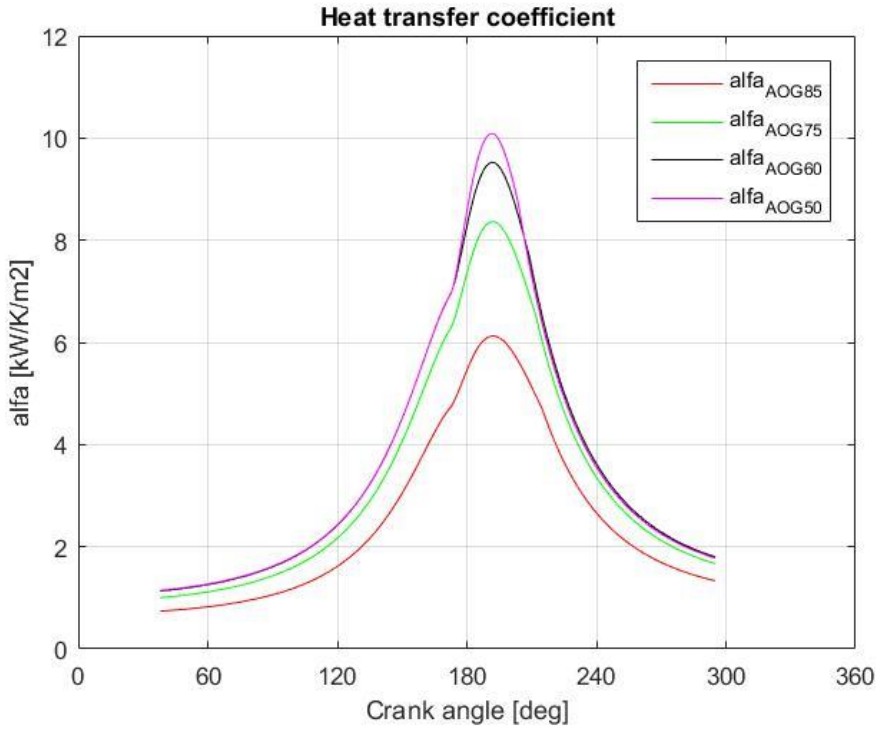

Figure 35: Heat transfer coefficient anode-off gasses

An overview of the simulation data for anode-off gas is given below in Table 19. For comparison reasons the data from producer gas is also shown.

Table 19: Results from simulation

Parameter	Units	**PG**	**AOG85**	**AOG75**	**AOG60**	**AOG50**
λ	-	0.925	1	1	1	1
CD	*° CA*	41	42.5	39.4	36.7	31.1
P_e	*kWe*	72.8	57.6	66.8	75.8	79.8
fc	*kg/h*	182	267	180	115.9	91
$\eta_{g\rightarrow e}$	-	0.28	0.16	0.17	0.19	0.20
Peak P	*Bar*	76.4	67.9	80.5	91.9	104.1
PoPP	*° CA*	13.2	12.4	12.3	12	11
Peak T	*K*	2111	2652	2651	2699	2847
σ	-	1.43	0.88	1.53	2.67	3.56
S_L	*m/s*	0.50	0.34	0.68	1.01	1.91

6-3 Analysis of results

Looking at the results there are several parameters that stand out. The important ones will be discussed in further detail.

6-3-1 Temperature

The temperature for anode-off gas is much higher (500-700 K) than producer gas. The peak temperature is in the range of 2650-2850 K. There are several reasons for the increase in temperature. One of them is the H_2 content in anode-off gas. H_2 has a high adiabatic flame temperature. At ambient conditions, the adiabatic flame temperature is 2367 K. However, after the inlet valve closes, the pressure and temperature rise. At the start of combustion, pressure and temperature are around 40 bar and 800 K respectively. At this pressure and temperature, the adiabatic flame temperature of H_2 increases to 2760 K [58]. At the same pressure and temperature, the adiabatic flame temperature of producer gas is 2260 K [43]. Increasing the H_2 content will thus increase the temperature as well. Also the large temperature increase can be explained by looking at how the temperature is calculated. The temperature follows from integrating the first law of thermodynamics:

$$\frac{dT}{dt} = \frac{\dot{Q}_{comb} - \dot{Q}_{loss} - p \cdot \frac{dV}{dt} + \dot{E}_f}{m \cdot c_v}$$

$\dot{Q}_{comb}$ is the mass times the LCV. In case of AOG85 compared to PG, the mass of fuel for AOG85 is larger than PG. Also, the LCV is higher, giving a higher $\dot{Q}_{comb}$. At the same time, the pressure is lower, so the term $p \cdot \frac{dV}{dt}$ is less. The c_v for AOG85 is much lower during combustion than for PG. When solving all the terms, the net results is that the temperature is higher for AOG85.

The high temperature could cause physical problems for the engine. The engine is a diesel engine converted for spark ignited operation. Normal operating temperatures for diesel engines are 1800-2300 K [59]. The temperatures for anode-off gas combustion are still much higher. Even though the peak temperature only occurs for a short period, such high temperatures might not be feasible in a combustion engine.

6-3-2 Pressure

With the increasing flame speed and LCV when using a lower utilization rate anode-off gas, the pressure increases as well. This is an expected trend, since pressure follows from the gas law:

$$p = \frac{mRT}{V}$$

Both R and T increase when using a lower utilization rate anode-off gas, where m and V stay relatively constant. As a result the pressure increases. The maximum pressure occurs using AOG50. The peak pressure is 104 bar. For small automotive diesel engines, which this engine could be categorized under, the typical peak pressure values are 120 bar [59]. The peak pressure is much higher than for PG, but still feasible.

6-3-3 Fuel consumption

The fuel consumption decreases toward a lower utilization rate anode-off gas. This is explained by the decreasing density and the increasing stoichiometric air/fuel ratio. The same volume in the cylinder will be filled under stoichiometric conditions. The lower density and higher air/fuel ratio cause the mass of fuel in the cylinder to decrease. Per cycle, less mass will be burned. Even though the fuel consumption decreases with lower utilization rate anode-off gas, the values should also be seen compared to conventional fuels. A similar size diesel engine with the same power output will use around 15 kg/h of fuel, which is six times lower than the lowest fuel consumption for anode-off gas. This questions also the feasibility of using anode-off gas for power generation.

6-3-4 Gas to electric efficiency

To compare the efficiencies of anode-off gas to producer gas, the indicated efficiencies are converted to efficiencies from gas to electric, taking into account the conversion efficiencies as discussed in chapter 5. Where producer gas still achieves a relatively good efficiency, the efficiencies for anode-off gas are poor, not even coming above 20%. This is the result of the relatively low power output for the fuel heat being added to the cylinder. The indicated efficiency is defined as:

$$\eta_i = \frac{W_i}{Q_f}$$

In which $Q_f = m_f \cdot LCV$ and the indicated work is calculated from the p-V curve. Even though anode-off gas is available as a by-product from the fuel cell and therefore "free" energy, the efficiency of the engine is poor and combusting this anode-off gas might not outweigh the costs of installing engines for anode-off gas combustion.

6-3-5 Position of peak pressure

The PoPP moves more toward the top dead center with lower utilization rates of anode-off gas. This is a direct effect of the faster laminar flame speed and thus shorter combustion duration. Anode-off gas combustion was tweaked such that it was at maximum brake torque timing. This timing can be checked by looking at the PoPP, which should be around 12-14° ATDC. To try and optimize the anode-off gas combustion, another round of simulations is done, ensuring the PoPP is similar to that of anode-off gas in the E6 engine.

6-4 Discussion on simulation results

This research was conducted with the aim of investigating the performance of an IC engine on different compositions of anode-off gas. A engine model has been adjusted and verified, after which it has been used to simulate anode-off gas combustion. During this process, assumptions have been made and several interesting results have been seen. Some of these need further clarification or discussion, which will happen in this section.

The above results from simulations show the potential that anode-off gas has for power generation when combusted in a SI engine. The engine used was originally a Diesel powered engine, rated at

100 kWe. The maximum power output achieved for anode-off gas was using AOG50, achieving almost 82 kWe. The power output seems reasonable. However, this power output is achieved at a temperature which may not be feasible for a combustion engine. Also the fuel consumption is minimum 6 times higher than using Diesel. When going to 85% fuel utilization the fuel consumption becomes almost 18 times as high as Diesel, with less than 60% of the power output. The availability of that much anode-off gas seems improbable, but should be further researched.

The peak temperature can be reduced by increasing the air excess ratio. Increasing this would lower the mixture LCV, lower the laminar flame speed, increase the combustion duration, and lower the peak pressure. The temperature would become feasible, but the drop in pressure would result in a drop in power output as well. Modelling anode-off gas at higher air excess ratios has not been included in this thesis. Several assumption that have been made in this study would not hold. The turbulence intensity would change, Vibe parameters would change which would alter the heat release profile, and the stoichiometric gas fraction from the previous cycle would change. It seems therefore very difficult to, without further experimental verification, use the same constant parameters in this study for higher air excess ratios.

The turbulence intensity is assumed constant over the crank angle, and is assumed to not change due to changes in composition when combustion takes place under stoichiometric conditions. In reality, turbulence intensity differs with crank angle, and will be influenced as well by changing composition due to different thermophysical properties. To research the specific effect of these changes, a 3D CFD model of the in-cylinder process containing the full chemical kinetics models should be build, solving the chemical reactions and simulating the turbulence due to engine geometry and speed.

In this study, the combustion duration has been related to the turbulent flame speed. The entire range from 0-90% has been modeled based on this relationship. In reality, the first and last phase of combustion are slower than the second phase. The approximation that has been used in this study is close to the experimental values, but is not exact.

One of the main differences with the original in-cylinder model for Diesel is the change to using Annand`s formulation for the heat loss. As explained before, this formulation incorporates the transport properties of the mixture much better then Woschni, who uses tunable coefficients. This way, the heat transfer coefficient is calculated more accurately, using NASA coefficients for individual species, ensuring a more correct heat loss model.

7 Conclusion and recommendations

7-1 Conclusions

In this thesis the performance of an IC engine running on anode-off gas has been investigated. This has been done to research if this can be used on board of ships for power generation. The research first focussed on modifying an engine model, after which it was used to simulate anode-off gas combustion. The key findings of this work are summarized in this chapter.

The first chapter presented the goal of this research, and outlined why this research is being conducted. The addition of anode-off gas to natural gas engines could broaden their engine envelope. Before this is done, combustion of anode-off gas needs to be researched. This has not yet been done, thus no data is available.

The second chapter looked at research on similar gasses. A similar gas to anode-off gas is producer gas. This can be used in both CI and SI engines. However, CI engines cannot run on 100% producer gas. SI engines have lower compression ratios which reduces power. Combustion of producer gas has proven possible at higher compression ratios by adopting a Diesel engine for SI operation. In research into combustion of synthesis gas in SI engines, most studies use a zero-dimensional model. Synthesis gas can have different heat release profiles depending on the composition of the gas. In order to correctly model the heat release, fuel specific Vibe parameters need to be used. It was found that the best way to model anode-off gas combustion, is using a SI engine in a in-cylinder model. When modeling the engine, ignition timing and fuel flow to the cylinder will have to be altered compared to CI simulation.

In chapter three the modifications to the Diesel-C model were discussed. The mass balance needs to be changed to account for the different mass balance in a gas engine. The model was made dependent of the different constituent volume percentages of anode-off gas. The formulation from Annand is used for the convective heat transfer coefficient to incorporate the different thermophysical properties of the different constituents better.

Chapter four matched the model to different experimental results from literature using producer gas as fuel. From 2 different engines enough experimental data was available to verify the model. The model was able to predict the pressure trace for both engines within an acceptable accuracy of 6%. For both the engines E6 TA and E4, the estimated peak load is only 2% and 8% off. The fuel consumption falls within a 2% margin. There was always an overestimation of the peak load, which can be caused by conversion losses which have not been taken into account. A 93% conversion efficiency from mechanical to electrical has been used to account for this overprediction. Based on

the simulation results, the model is found to work sufficiently and further investigation into anode-off gas can be done with the model.

In chapter five the behaviour of anode-off gas was examined in detail by looking at the laminar and turbulent flame speed and relating these to the combustion duration. It was discovered, when increasing the amount of hydrogen, that both the initial development phase and the fast burn phase were shortened. However the terminal phase takes longer. The terminal phase can be disregarded, when the combustion efficiency is assumed to be similar to producer gas (90%). The first two phases both seem to be turbulent. Therefore the total combustion duration can be linked to the turbulent flame speed, which is a function of laminar flame speed and turbulent intensity. Assuming the turbulent intensity to stay constant, the turbulent flame speed and the combustion duration can be calculated using the ratio of turbulent flame speeds between two gasses. The laminar flame speeds of anode-off gas and their combustion duration in engine E6 are given in Table 20.

Table 20: Calculated combustion duration and laminar flame speed for anode-off gas

	Combustion duration 0-90% of mass burn fraction, given in crank angle	**Laminar flame speed at stoichiometry (m/s)**
PG	41	0.5
AOG,85	42.5	0.34
AOG,75	39.4	0.68
AOG,60	36.7	1.01
AOG,50	31.1	1.91

Chapter six presented and analysed the results of modelling anode-off gas combustion. Several parameters have been kept constant to be able to compare anode-off gas to producer gas. These parameters are engine geometry, air excess ratio, T_1, p_1, Vibe parameters and stoichiometric gas mass fraction from the previous cycle. At first the SOC is kept constant as well, only altering the EOC for different combustion durations. The maximum power output is 78.9 kWe for AOG50. The maximum efficiency is 20%. The peak pressure is 104 bar, which is higher than for producer gas, but falls within the limits of what the engine can handle. The peak temperature is 2847 K, which is more than 700 K higher than producer gas. The engine, it is believed, can not handle this. The lowest peak temperature is reached for AOG85 and is 2652 K. This is still outside normal engine operating temperatures. Combustion of anode-off gas under stoichiometric conditions in an IC engine is therefore not feasible. Increasing the air excess ratio could resolve this issue, but can not be done in the current model without having experimental data on anode-off gas. The fuel consumption is 6-18 times higher than conventional fuels, also showing that anode-off gas combustion would not be an advantage over conventional fuels. More power at lower temperatures can be reached when retarding start of combustion, achieving MBT timing. Peak power is achieved using AOG50 and is 81.6 kWe. The corresponding peak temperature is 2822 K, which is also outside normal operating conditions of IC engines.

7-2 Recommendations

The modelling investigation in this thesis has provided a basic understanding of combustion of anode-off gas in an IC engine and its implications. An engine model was modified and verified. However, the model is limited in its use and several assumption needed to be made.

One of the potential improvements is to get a better relation for flame speed and combustion duration. With a 3D CFD model, more accurate predictions could be made, and no linearization would have to be used. Also a more detailed investigation into the different combustion phases and their turbulence would be beneficial for this work.

Another potential improvement would be to achieve anode-off gas specific Vibe coefficients. The easiest way to do this would be to do experimental investigations into anode-off gas combustion.

With experimental investigations, combustion of anode-off gas can also be researched at different air excess ratios. With this data, the model could be further developed to also work at different air excess ratios, which is now not the case yet.

Lastly, further research could be done into a better relation for the influence of turbulence intensity in the cylinder at different crank angles. In this work, the turbulent intensity is kept constant over the crank angle. However, in reality this differs slightly which causes different flame speeds and combustion durations.

References

[1] B. Basu, Biomass Gasification and Pyrolysis: Practical Design and Theory, New York: Elsevier, 2010.

[2] S. Dasappa en H. Sridhar, „Experiments on and thermodynamic analysis of a turbocharged engine with producer gas as fuel," *Mechanical Engineering Science,* 2012.

[3] P. Raman en N. Ram, „Performance analysis of an internal combustion engine operated on producer gas, in comparison with the performance of the natural gas and diesel engines," *Energy,* pp. 317-333, 2013.

[4] P. Gobbato, M. Masi en M. Benetti, „Performance analysis of a producer gas-fuelled heavy-duty SI engine at full-load operation," in *ATI 2015 - 70th Conference of the ATI Engineering Association*, 2015.

[5] A. Shivapuji en S. Dasappa, „Selection and thermodynamic analysis of a turbocharger for a producer gas-fuelled multi-cylinder engine," *Journal of power and energy,* pp. 340-356, 2014.

[6] F. Hagos, A. Rashid A. Aziz en S. Sulaiman, „Trends of SYngas as a Fuel in Internal Combustion Engines," *Advances in Mechanical Engineering,* 2014.

[7] A. Boehman en O. Le Corre, „Combustion of Syngas in Internal Combustion Engines," *Combustion Science and Technology,* pp. 1193-1206, 2008.

[8] B. Sahoo, U. Saha en N. Sahoo, „Theoretical performance limits of a syngas-diesel fueled compression ignition engine from second law analysis," *Energy*, pp. 760-769, 2011.

[9] B. Sahoo, N. Sahoo en U. Saha, „Effect of H2:CO ratio in syngas on the performance of a dual fuel diesel engine operation," *Applied Thermal Engineering,* pp. 139-146, 2011.

[10] B. Sahoo, U. Saha en N. Sahoo, „Effect of Load Level on the Performance of a Dual Fuel Compression Ignition Engine Operating on Syngas Fuels With Varying H2/CO Content," *Journal of Engineering for Gas Turbines and Power,* pp. 122802-1-122802-12, 2011.

[11] C. Spaeth, „Performance characterisitcs of a diesel fuel piloted syngas compression ignition engine," Department of Mechanical and Materials Engineering, Queen's University, Kingston, Canada, 2012.

[12] G. Sridhar en R. Babu Yarasu, „Facts about producer gas engine," in *Paths to sustainable energy*, InTech, 2010, pp. 537-560.

[13] A. Shah, R. Srinivasan, S. Filip To en E. Columbus, „Peformance and emissions of a spark-ignited engine driven generator on biomass based syngas," *Bioresource Technology,* pp. 4656-4661, 2010.

[14] A. Shivapuji en S. Dasappa, „Experimental Studies on Multi-Cylinder Natural Gas Engine Fueled with Producer Gas," in *19th European Biomass Conference and Exhibition*, Berlin, Germany, 2011.

[15] S. Dasappa, „On the estimation of power froma diesel engine converted for gas operation – a simple analysis,” in *Proceedings of the seventeenth national conference on I.C. engines and combustion*, Bangalore, India, 2001.

[16] Mustafi, N.N., Y. Miraglia, R. Raine, P. Bansal and S. Elder, "Spark-ignition engine performance with 'Powergas' fuel (mixture of CO/H2): A comparison with gasoline and natural gas," *Fuel 85*, pp. 1605-1612, 2006.

[17] P. Raman en N. Ram, „Performance analysis of an internal combustion engine operated on producer gas, in comparison with the performance of the natural gas and diesel engines,” *Energy*, pp. 317-333, 2013.

[18] B. Mahgoub, S. Sulaiman en Z. Karim, „Performance study of imitated syngas in a dual-fuel compression ignition diesel engine,” *International journal of Automotive and Mechanical Engineering*, vol. 2015, nr. Volume 11, pp. 2282-2293, 2015.

[19] V. Sobyanin, V. Sadykov, V. Kirillov, V. Kuzmin, N. Kuzin, Z. Vostrikov, E. Smirnov, A. Sorokin, O. Brizitskiy, V. Terentyev, A. Khristolyubov, V. Luksho en A. Afanasiev, „Syngas As A Fuel For IC And Diesel Engines: Efficiency And Harmful Emissions cut-off,” in *Proceedings International Hydrogen Energy Congress and Exhibition IHEC 2005*, Istanbul, Turkey, 2005.

[20] P. Schulten, „The interaction between diesel engines, ship and propellers during manoeuvring,” Delft, 2005.

[21] D. Stapersma, „Diesel engines modelling strategies,” in *Diesel Engines Volume 2 Turbocharging*, Delft, 2010, p. 427.

[22] Y. Ding, „Characterising Combustion in Diesel Engines,” Delft, 2011.

[23] M. Costa, M. La Villeta, N. Massarotti, D. Piazzullo en V. Rocco, „Numerical analysis of a compression ignition engine powered in the dual-fuel mode with syngas and biodiesel,” *Energy*, vol. 2017, pp. 1-11, 2017.

[24] B. Gamino en J. Aguillon, „Numerical simulation of syngas combustion multi-spark ignition system in a diesel engine adapted to work at the Otto cycle,” *Fuel*, vol. 2010, pp. 581-591, 2009.

[25] F. Zhang, R. Yu en X. Bai, „Detailed numerical simulation of syngas combustion under partially premixed combustion engine conditions,” *International Journal of Hydrogen Energy*, vol. 2012, nr. 37, pp. 17285-17293, 2012.

[26] H. Sapra, M. Godjevac, K. Visser, D. Stapersma en C. Dijkstra, „Experimental and simulation-based investigations of marine diesel engine performance against static back pressure,” *Applied Energy*, vol. 2017, nr. 204, pp. 78-92, 2017.

[27] R. Geertsma, R. Negenborn, K. Visser, M. Loonstijn en J. Hopman, „Pitch control for ships with diesel mechanical and hybrid propulsion: Modelling, validation and performance quantification,” *Applied Energy*, vol. 2017, nr. 206, pp. 1609-1631, 2017.

[28] G. Merker, C. Schwarz, G. Stiesch en .. Otto, Simulating Combustion, Germany: Springer, 2006.

[29] F. Baldi, G. Theotokatos en K. Andersson, „Development of a combined mean value-zero dimensional model and application for a large marine four-stroke Diesel engine simulation,” *Applied Energy*, vol. 2015, nr. 154, pp. 402-415, 2015.

[30] H. Grimmelius, E. Mesbahi, P. Schulten en D. Stapersma, „The use of diesel engine simulation models in ship propulsion plant design and operation," in *25th CIMAC WC*, Vienne, Austria, 2007.

[31] P. Schulten en D. Stapersma, „Mean value modelling of the gas exchange of a 4-stroke diesel engine for use in powertrain applications," in *SAE 2003 World Congress & Exhibition*, United States, 2003.

[32] C. Dijkstra, „Mean value diesel engine model for simulating the off-design performance of 2 and 4 stroke diesel engines," Delft University of Technologie, Delft, 2003.

[33] I. Georgescu, „Characterizing the Transient Behaviour of Dual-Fuel Engines by Adapting a Diesel Engine Model," Delft University of Technology, Delft.

[34] G. Woschni, „A universally applicable equation for the instantaneous heat transfer coefficient in the internal combustion engine," SAE, United States, 1967.

[35] G. Merker, B. Hohlbaum en M. Rausher, „Two-zone model for calculation of nitrogen-oxide formation in direct-injection diesel engines," SAE, United States, 1993.

[36] Y. Linden, „NO-emission prediction in a Diesel engine using a two zone in-cylinder simulation model," Delft university of Technology, Delft, 2017.

[37] S. Lopez, „Three-Zone in cylinder process model for DI diesel engines," Delft University of Technology, Delft, 2014.

[38] G. Theotokatos, „A Comparative Study on Mean Value Modelling of Two-Stroke Marine Diesel Engine," in *Proceedings of the 2nd International Conference on Maritime and Naval Science and Engineering*, Greece, 2010.

[39] Y. Tang, J. Zhang, H. Gan, B. Jia en Y. Xia, „Development of a real-time two-stroke marine diesel engine model with in-cylinder pressure prediction capability," *Applied Energy*, vol. 2017, nr. 194, pp. 55-70, 2017.

[40] G. Sridhar, P. Paul en H. Mukunda, „Zero-dimensional modelling of a producer gas-based reciprocating engine," *Power and Energy,* vol. 2006, nr. 220, pp. 923-931, 2006.

[41] C. Rakopoulos en C. Michos, „Development and validation of a multi-zone combustion model for performance and nitric oxide formation in syngas fueled spark ignition engine," *Energy Conversion and Management,* vol. 2008, nr. 49, pp. 2924-2938, 2008.

[42] A. Shivapuji en S. Dasappa, „Experiments and zero D modeling studies using specific Wiebe coefficients for producer gas as fuel in spark-ignited engines," *J Mechanical Engineering Science*, vol. 2012, nr. 227(3), pp. 504-519, 2012.

[43] A. Shivapuji, „In-cylinder experimental and modeling studies on producer gas fuelled operation of spark ignited gas engines," Center for Sustainable Technologies Indian Institute of Science , India, 2015.

[44] D. Stapersma, Diesel Engines Volume 1, performance analysis, Delft: Delft University of Technology, 2010.

[45] J. B. Heywood, Internal combustion engine fundamentals, New York: McGraw-Hill, 1988.

[46] T. A. Davidson, „A Slmple and Accurate Method for Calculatlng Viscosity of Gaseous Mixtures," United States department of the interior, bureau of mines, Spokane, United States, 1993.

[47] C. Wilke, „A viscosity equation for gas mixtures," *The Journal of Chemical Physics,* vol. 1950, nr. 4, pp. 517-519, 1950.

[48] R. E. Svehla, „Transport coefficients for the NASA Lewis Chemical Equilibrium Program," NASA, Cleveland, Ohio, 1995.

[49] R. Sridhar, „Experiments and Modelling Studies of Producer Gas based Spark-Ignited Reciprocating Engines," Indian Institute of Science, Department of Aerospace Engineering, Bangalore, India, 2005.

[50] J. C. Keck, J. B. Heywood en G. Noske, „Early Flame Developments and Burning Rates in Spark Ignition Engines and their Cyclic Variability," SAE, Detroit, Michigan, 1987.

[51] V. Kurdyumov, J. Blasco, A. Sanchez en A. Linan, „On the calculation of the minimum ignition energy," *Combustion and flame,* nr. 136, pp. 394-397, 2004.

[52] D. Roekaerts, Interviewee, *laminar/turbulent flames in SI engines.* [Interview]. 8 6 2018.

[53] B. Ravindra, „PREMIXED TURBULENT COMBUSTION OF PRODUCER GAS IN CLOSED VESSEL AND ENGINE CYLINDER," Indian institute of Science, Bangalore, 2009.

[54] S. Chakravarthy, „Module 7, lecture 27, Laminar premixed flames," Madras, India, 2016.

[55] P. Siewert, „Flame front characteristics of turbulent lean premixed methane / air flames at high-pressure," PUT, Poznan, Poland, 2006.

[56] G. Damkohler, „Der Einfluß der Turbulenz auf die Flammengeschwindigkeit in Gasgemischen," *Zeitshrift fur Elektrochemie und Angewandte Physikalische Chemie,* vol. 1940, nr. 11, pp. 601-652, 1940.

[57] S. RAO, „Experiments and modelling studies of producer gas based spark ignited reciprocating engines," Indian institute of Science, Bangalore, 2003.

[58] D. Lapalme en P. Seers, „Influence of CO2, CH4, and initial temperature on H2/CO laminar flame speed," *Hydrogen Energy,* vol. 2014, nr. 39, pp. 3477-3486, 2014.

[59] G. Stiesch, Modeling Engine Spray and Combustion Processes, Hannover, Germany: Springer Science & Business Media, 2013.

[60] Cerfacs, „Elearning at Cerfacs, Adiabatic Flame Temperature Calculator," [Online]. Available: http://elearning.cerfacs.fr/combustion/tools/adiabaticflametemperature/index.php. [Geopend 15 6 2018].

[61] R. P. Bates en K. Dölle, „Syngas use in Internal Combustion Engines - A Review," *Advances in Research,* 2017.

[62] R. Stephen, An introduction to combustion: concepts and applications, Europe: Mcgraw-Hill Education , 2011.